MDPI

Article

Using Timeliness in Tracking Infections †

Melih Bastopcu [1] and Sennur Ulukus [2],*

1   Coordinated Science Laboratory, University of Illinois Urbana-Champaign, Urbana, IL 61801, USA; bastopcu@illinois.edu
2   Department of Electrical and Computer Engineering, University of Maryland, College Park, MD 20742, USA
*   Correspondence: ulukus@umd.edu
†   This paper is an extended version of our paper published in 2021 IEEE INFOCOM 2021—IEEE International Conference on Computer Communications (online), 10–13 May 2021.

Abstract: We consider real-time timely tracking of infection status (e.g., COVID-19) of individuals in a population. In this work, a health care provider wants to detect both infected people and people who have recovered from the disease as quickly as possible. In order to measure the timeliness of the tracking process, we use the long-term average difference between the actual infection status of the people and their real-time estimate by the health care provider based on the most recent test results. We first find an analytical expression for this average difference for given test rates, infection rates and recovery rates of people. Next, we propose an alternating minimization-based algorithm to find the test rates that minimize the average difference. We observe that if the total test rate is limited, instead of testing all members of the population equally, only a portion of the population may be tested in unequal rates calculated based on their infection and recovery rates. Next, we characterize the average difference when the test measurements are erroneous (i.e., noisy). Further, we consider the case where the infection status of individuals may be dependent, which occurs when an infected person spreads the disease to another person if they are not detected and isolated by the health care provider. In addition, we consider an age of incorrect information-based error metric where the staleness metric increases linearly over time as long as the health care provider does not detect the changes in the infection status of the people. Through extensive numerical results, we observe that increasing the total test rate helps track the infection status better. In addition, an increased population size increases diversity of people with different infection and recovery rates, which may be exploited to spend testing capacity more efficiently, thereby improving the system performance. Depending on the health care provider's preferences, test rate allocation can be adjusted to detect either the infected people or the recovered people more quickly. In order to combat any errors in the test, it may be more advantageous for the health care provider to not test everyone, and instead, apply additional tests to a selected portion of the population. In the case of people with dependent infection status, as we increase the total test rate, the health care provider detects the infected people more quickly, and thus, the average time that a person stays infected decreases. Finally, the error metric needs to be chosen carefully to meet the priorities of the health care provider, as the error metric used greatly influences who will be tested and at what test rate.

Keywords: timely infection tracking; age of information; timely tracking of multiple processes; Markovian infection spread model

1. Introduction

We consider the problem of timely tracking of an infectious disease, e.g., COVID-19, in a population of n people. In this problem, a health care provider wants to detect infected people as quickly as possible in order to take precautions such as isolating them from the rest of the population. The health care provider also wants to detect people who have recovered from the disease as soon as possible since these people need to return to work which is especially critical in sectors such as education, food retail, public transportation,

etc. Ideally, the health care provider should test all people all the time. However, as the total test rate is limited, the question is how frequently the health care provider should apply tests on these people when their infection and recovery rates are known. In a broader sense, this problem is related to timely tracking of multiple processes in a resource-constrained setting where each process takes binary values of 0 and 1 with different change rates.

Recent studies have shown that people who have recovered from infectious diseases such as COVID-19 can be reinfected. Furthermore, the recovery times of individuals may vary significantly. For these reasons, in this problem, the *i*th person becomes infected with rate λ_i which is independent of the others. Similarly, the *i*th person recovers from the disease with rate μ_i. We note that the index *i* may represent a specific individual or a group of individuals that share common features such as age, gender, and profession. Depending on the demographics, coefficients λ_i and μ_i may be statistically known by the health care provider. We denote the infection status of the *i*th person as $x_i(t)$ (shown with the black curves on the left in Figure 1) which takes the value 1 when the person is infected and the value 0 when the person is healthy. The health care provider applies tests to people marked as healthy with rate s_i and to people marked as infected with rate c_i. Based on the test results, the health care provider forms an estimate for the infection status of the *i*th person denoted by $\hat{x}_i(t)$ (shown with the blue curves on the right in Figure 1) which takes the value 1 when the most recent test result is positive and the value 0 when it is negative.
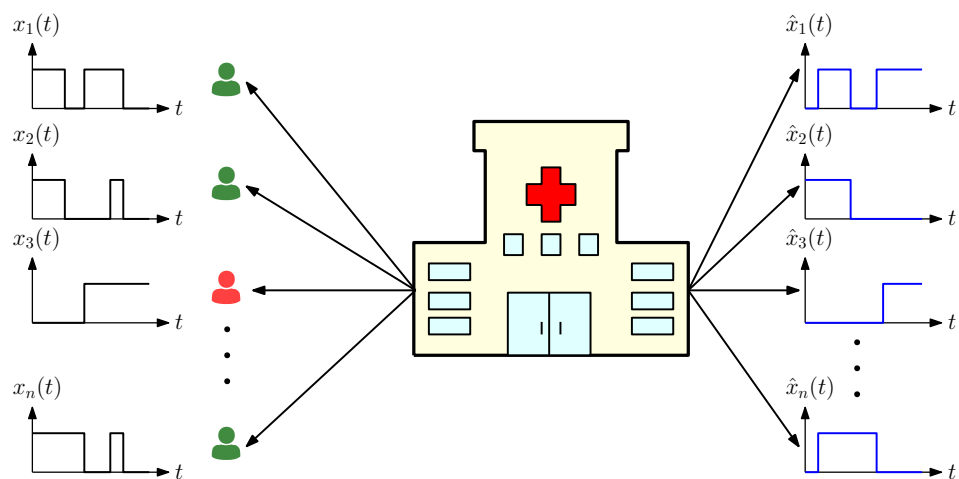

Figure 1. System model. There are *n* people whose infection status are given by $x_i(t)$. The health care provider applies tests on these people. Based on the test results, estimations for the infection status $\hat{x}_i(t)$ are generated. Infected people are shown in red and healthy people are shown in green.

We measure the timeliness of the tracking process by the difference between the actual infection status of people and the real-time estimate of the health care provider which is based on the most recent test results. The difference can occur in two different cases: (i) when the person is sick ($x_i(t) = 1$) and the health care provider maps this person as healthy ($\hat{x}_i(t) = 0$), and (ii) when the person recovers from the disease ($x_i(t) = 0$) but the health care provider still considers this person as infected ($\hat{x}_i(t) = 1$). The former case represents the error due to late detection of infected people, while the latter case represents the error due to late detection of healed people. Depending on the health care provider's preferences, detecting infected people may be more important than detecting recovered people (controlling infection), or the other way around (returning people to workforce).

The age of information was proposed to measure timeliness of information in communication systems, and has been studied in the context of queueing systems [1–8], multi-hop and multi-cast networks [9–17], social networks [18], timely remote estimation of random processes [19–25], energy harvesting systems [26–40], wireless fading channels [41,42], scheduling in networks [43–55], lossless and lossy source and channel coding [56–66], vehicular, IoT and UAV systems [67–70], caching systems [71–82], computation-intensive systems [83–90], learning systems [91–93], gossip networks [94–97] and so forth. A more

detailed review of the age of information literature can be found in references [98–100]. Most relevant to our work, the real-time timely estimation of single and multiple counting processes [19,25], a Wiener process [20], a random walk process [101], and binary and multiple states Markov sources [23,51,102] have been studied. The study that is closest to our work is reference [23], where the remote estimation of a symmetric binary Markov source is studied in a time-slotted system by finding the optimal sampling policies via formulating a Markov Decision Process (MDP) for real-time error, AoI and AoII metrics. Different from [23], in our work, we consider real-time timely estimation of multiple non-symmetric binary sources for a continuous time system. In our work, the sampler (health care provider) does not know the states of the sources (infection status of people), and thus, takes the samples (applies medical tests) randomly (exponential random variables) with fixed rates. Thus, we optimize the test rates of people to minimize the real-time estimation error.

In this paper, we consider the real-time timely tracking of infection status of n people. We first find an analytical expression for the long-term average difference between the actual infection status of people and the estimate of the health care provider based on test results. Then, we propose an alternating minimization-based algorithm to identify the test rates s_i and c_i for all people. We observe that if the total test rate is limited, we may not apply tests on all people equally. Next, we provide an alternative method to characterize the average difference, by finding the steady state of a Markov chain defined by $(x_i(t), \hat{x}_i(t))$. By using this alternative method, we determine the average estimation error when there are errors in the test measurements expressed by a false positive rate p and a false negative rate q. Next, we consider the infection status of two people where an infected person may spread the disease to another person if the infection has not been detected by the health care provider to consequently isolate the infected person. Finally, we consider an age of incorrect information-based error metric where the estimation error increases linearly over time when the health care provider has not detected the changes in the infection status of the people.

Through extensive numerical results, we observe that increasing the total test rate helps track the infection status of people better, and increasing the size of the population increases diversity which may be exploited to improve the performance. Depending on the health care provider's priorities, we can allocate additional tests to people marked as healthy to detect the infections faster or to people marked as infected to detect the recoveries more quickly. In order to combat the test errors, the health care provider may prefer to apply tests to only a selected portion of the population with higher test rates. When the infection status of a person depends on that of another person, the average time that a person remains infected can be reduced by increasing the total test rate as it helps to detect the infected people more quickly. Finally, we observe that depending on the error metric used, the test rate distribution among the population differs greatly, and thus, we should choose an error metric that aligns with the priorities of the health care provider.

2. System Model

We consider a population of n people. We denote the infection status of the ith person at time t as $x_i(t)$ (black curve in Figure 2a) which takes binary values 0 or 1 as follows,

$$x_i(t) = \begin{cases} 1, & \text{if the } i\text{th person is infected at time } t, \\ 0, & \text{otherwise.} \end{cases} \tag{1}$$

In this paper, we consider a model where each person can be infected multiple times after recovering from the disease. We denote the time interval that the ith person stays healthy for the jth time as $W_i(j)$ which is exponentially distributed with rate λ_i. We denote the recovery time for the ith person after being infected with the virus for the jth time as $R_i(j)$ which is exponentially distributed with rate μ_i.

A health care provider wants to track the infection status of each person. Based on the test results at times $t_{i,\ell}$, the health care provider generates an estimate for the status of the ith person denoted as $\hat{x}_i(t)$ (blue curve in Figure 2a) by

$$\hat{x}_i(t) = x_i(t_{i,\ell}), \quad t_{i,\ell} \leq t < t_{i,\ell+1}. \tag{2}$$

When $\hat{x}_i(t)$ is 1, the health care provider applies the next test to the ith person after an exponentially distributed time with rate c_i. When $\hat{x}_i(t)$ is 0, the next test is applied to the ith person after an exponentially distributed time with rate s_i.
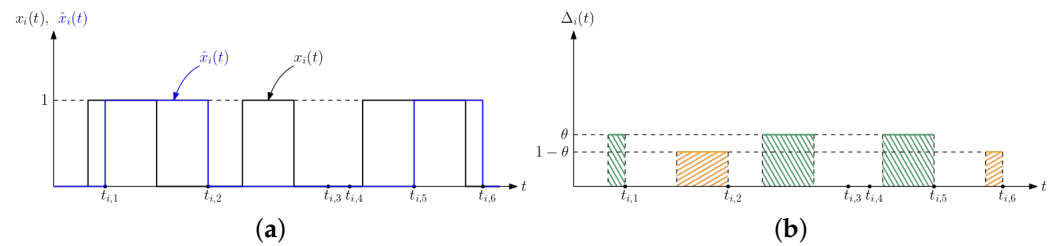

Figure 2. (**a**) A sample evolution of $x_i(t)$ and $\hat{x}_i(t)$, and (**b**) the corresponding $\Delta_i(t)$ in (5). Green areas correspond to the error caused by $\Delta_{i1}(t)$ in (3). Orange areas correspond to the error caused by $\Delta_{i2}(t)$ in (4).

An estimation error happens when the actual infection status of the ith person, $x_i(t)$, is different than the estimate of the health care provider, $\hat{x}_i(t)$, at time t. This could happen in two ways: when $x_i(t) = 1$ and $\hat{x}_i(t) = 0$, i.e., when the ith person is sick, but remains undetected by the health care provider, and when $x_i(t) = 0$ and $\hat{x}_i(t) = 1$, i.e., when the ith person has recovered, but the health care provider is unaware that the ith person has recovered.

We denote the error caused by the former case, i.e., when $x_i(t) = 1$ and $\hat{x}_i(t) = 0$, by $\Delta_{i1}(t)$ (green areas in Figure 2b),

$$\Delta_{i1}(t) = \max\{x_i(t) - \hat{x}_i(t), 0\}, \tag{3}$$

and we denote the error caused by the latter case, i.e., when $x_i(t) = 0$ and $\hat{x}_i(t) = 1$, by $\Delta_{i2}(t)$ (orange areas in Figure 2b),

$$\Delta_{i2}(t) = \max\{\hat{x}_i(t) - x_i(t), 0\}. \tag{4}$$

Then, the total estimation error for the ith person $\Delta_i(t)$ is

$$\Delta_i(t) = \theta \Delta_{i1}(t) + (1 - \theta)\Delta_{i2}(t), \tag{5}$$

where θ is the importance factor in $[0, 1]$. A large θ gives more importance to the detection of infected people, and a small θ gives more importance to the detection of recovered people.

We define the long-term weighted average difference between $x_i(t)$ and $\hat{x}_i(t)$ as

$$\Delta_i = \lim_{T \to \infty} \frac{1}{T} \int_0^T \Delta_i(t) dt. \tag{6}$$

Then, the overall average difference of all people Δ is

$$\Delta = \frac{1}{n} \sum_{i=1}^n \Delta_i. \tag{7}$$

Our aim is to track the infection status of all people. Due to limited resources, there is a total test rate constraint $\sum_{i=1}^n s_i + \sum_{i=1}^n c_i \leq C$. Thus, our aim is to find the optimal

test rates s_i and c_i to minimize Δ in (7) while satisfying this total test rate constraint. We formulate the following problem,

$$\min_{\{s_i,c_i\}} \quad \Delta$$

$$\text{s.t.} \quad \sum_{i=1}^{n} s_i + \sum_{i=1}^{n} c_i \leq C$$

$$s_i \geq 0, \quad c_i \geq 0, \quad i = 1, \dots, n. \tag{8}$$

We provide a summary of the list of the variables used in this work in Table 1. In the next section, we find the total average difference Δ.

Table 1. List of variables used in this work.

Variables	Definition of the Variables
Sections 2–4	
n	number of people in the population
$x_i(t)$	infection status of the ith person at time t
$\hat{x}_i(t)$	estimation of $x_i(t)$ at the health care provider
λ_i, μ_i	infection and recovery rates for the ith person
c_i, s_i	test rates applied to the ith person when $\hat{x}_i(t) = 1$, and $\hat{x}_i(t) = 0$
$\Delta_i(t)$	total estimation error for the ith person at time t
θ	importance factor in $[0, 1]$
Δ_i	the long-time weighted average for the ith person
C	total test rate constraint
Section 5	
Δ_i^e	the long-time average difference for the ith person with erroneous test measurements
q	false-negative testing probability with $0 \leq q < \frac{1}{2}$
p	false-positive testing probability with $0 \leq p < \frac{1}{2}$
v_i	test rate applied to the ith person with erroneous test measurements
Section 6	
λ, μ	individual infection and recovery rate of a person
λ_{12}	the rate of spreading the virus from an undetected infected person to a healthy person
c, s	test rates applied to people when $\hat{x}_i(t) = 1$, and $\hat{x}_i(t) = 0$
Δ_i^d	the long-time average difference for the ith person with dependent infection rates
Section 7	
w_i	test rate applied to the ith person for AoII-based error metric
Δ_i^s	the long-time average difference for the ith person with AoII-based error metric

3. Average Difference Analysis

In this section, we provide a probabilistic analysis to characterize the average difference Δ. In Section 5.1, we give an alternative method to find Δ by analyzing the steady-state

distribution of the Markov chain induced by the states $(x_i(t), \hat{x}_i(t))$. Here, we first find analytical expressions for $\Delta_{i1}(t)$ in (3) and $\Delta_{i2}(t)$ in (4) when $s_i > 0$ and $c_i > 0$. We note that $\Delta_{i1}(t)$ can be equal to 1 when $\hat{x}_i(t) = 0$ and is always equal to 0 when $\hat{x}_i(t) = 1$. Assume that at time 0, both $x_i(0)$ and $\hat{x}_i(0)$ are 0. After an exponentially distributed time with rate λ_i, which is denoted by W_i, the ith person is infected, and thus $x_i(t)$ becomes 1. At that time, since $\hat{x}_i(t) = 0$, $\Delta_{i1}(t)$ becomes 1. Further, $\Delta_{i1}(t)$ will be equal to 0 again either when the ith person recovers from the disease which happens after R_i which is exponentially distributed with rate μ_i or when the health care provider performs a test on the ith person after D_i, which is exponentially distributed with rate s_i. We define $T_m(i)$ as the earliest time at which one of these two cases happens, i.e., $T_m(i) = \min\{R_i, D_i\}$ (which is shown by the green areas in Figure 3a). We note that $T_m(i)$ is also exponentially distributed with rate $\mu_i + s_i$, and we have $\mathbb{P}(T_m(i) = R_i) = \frac{\mu_i}{\mu_i + s_i}$ and $\mathbb{P}(T_m(i) = D_i) = \frac{s_i}{\mu_i + s_i}$. If the ith person recovers from the disease before testing, we return to the initial case where both $x_i(t)$ and $\hat{x}_i(t)$ are equal to 0 again. In this case, the cycle repeats itself, i.e., the ith person becomes sick again after W_i and $\Delta_{i1}(t)$ remains as 1 until either the person recovers or the health care provider performs a test which takes another $T_m(i)$ duration. If the health care provider performs a test before the person recovers, then $\hat{x}_i(t)$ becomes 1. We denote the time interval for which $\hat{x}_i(t)$ stays at 0 as I_{i1} which is given by

$$I_{i1} = \sum_{\ell=1}^{K_1} T_m(i, \ell) + W_i(\ell), \tag{9}$$

where K_1 is geometric with rate $\mathbb{P}(T_m(i) = D_i) = \frac{s_i}{\mu_i + s_i}$. Due to [103] (Prob. 9.4.1), $\sum_{\ell=1}^{K_1} T_m(i, \ell)$ and $\sum_{\ell=1}^{K_1} W_i(\ell)$ are exponentially distributed with rates s_i and $\frac{\lambda_i s_i}{\mu_i + s_i}$, respectively. As $\mathbb{E}[I_{i1}] = \mathbb{E}[\sum_{\ell=1}^{K_1} T_m(i, \ell)] + \mathbb{E}[\sum_{\ell=1}^{K_1} W_i(\ell)]$, we have

$$\mathbb{E}[I_{i1}] = \frac{1}{s_i} + \frac{s_i + \mu_i}{s_i \lambda_i}. \tag{10}$$

When $\hat{x}_i(t) = 1$, the health care provider marks the ith person as infected. The ith person recovers from the virus after R_i. After the ith person recovers, either the health care provider performs a test after Z_i which is exponentially distributed with rate c_i or the ith person is reinfected with the virus which takes W_i time. We define $T_u(i)$ as the earliest time at which one of these two cases happens, i.e., $T_u(i) = \min\{W_i, Z_i\}$ (which is shown by the orange areas in Figure 3b). Similarly, we note that $T_u(i)$ is exponentially distributed with rate $\lambda_i + c_i$, and we have $\mathbb{P}(T_u(i) = W_i) = \frac{\lambda_i}{\lambda_i + c_i}$ and $\mathbb{P}(T_u(i) = Z_i) = \frac{c_i}{\lambda_i + c_i}$. If the person is reinfected with the virus before a test is applied, this cycle repeats itself, i.e., the ith person recovers after another R_i, and then either a test is applied to the ith person, or the person is infected again which takes another $T_u(i)$. If the health care provider performs a test to the ith person before the person is reinfected, the health care provider marks the ith person as healthy again, i.e., $\hat{x}_i(t)$ becomes 0. We denote the time interval that $\hat{x}_i(t)$ is equal to 1 as I_{i2} which is given by

$$I_{i2} = \sum_{\ell=1}^{K_2} T_u(i, \ell) + R_i(\ell), \tag{11}$$

where K_2 is geometric with rate $\mathbb{P}(T_u(i) = Z_i) = \frac{c_i}{\lambda_i + c_i}$. Similarly, $\sum_{\ell=1}^{K_2} T_u(i, \ell)$ and $\sum_{\ell=1}^{K_2} R_i(\ell)$ are exponentially distributed with rates c_i and $\frac{c_i \mu_i}{\lambda_i + c_i}$, respectively. As $\mathbb{E}[I_{i2}] = \mathbb{E}[\sum_{\ell=1}^{K_2} T_u(i, \ell)] + \mathbb{E}[\sum_{\ell=1}^{K_2} R_i(\ell)]$, we have

$$\mathbb{E}[I_{i2}] = \frac{1}{c_i} + \frac{c_i + \lambda_i}{c_i \mu_i}. \tag{12}$$

We denote the time interval between the jth and $(j+1)$th times that $\hat{x}_i(t)$ changes from 1 to 0 as the jth cycle $I_i(j)$ where $I_i(j) = I_{i1}(j) + I_{i2}(j)$. We note that $\Delta_{i1}(t)$ is always equal to 0 during $I_{i2}(j)$, i.e., $\hat{x}_i(t) = 1$, and $\Delta_{i1}(t)$ is equal to 1 when $x_i(t) = 1$ in $I_{i1}(j)$. We denote the total time duration when $\Delta_{i1}(t)$ is equal to 1 as $T_{e,1}(i,j)$ during the jth cycle where $T_{e,1}(i,j) = \sum_{\ell=1}^{K_1} T_m(i,\ell)$. Thus, we have $\mathbb{E}[T_{e,1}(i)] = \frac{1}{s_i}$. Then, using ergodicity, similar to [80], Δ_{i1} is equal to

$$\Delta_{i1} = \frac{\mathbb{E}[T_{e,1}(i)]}{\mathbb{E}[I_i]} = \frac{\mathbb{E}[T_{e,1}(i)]}{\mathbb{E}[I_{i1}] + \mathbb{E}[I_{i2}]}. \tag{13}$$

Thus, we have

$$\Delta_{i1} = \frac{\mu_i \lambda_i}{\mu_i + \lambda_i} \frac{c_i}{\mu_i c_i + \lambda_i s_i + c_i s_i}. \tag{14}$$

Next, we find Δ_{i2}. We note that $\Delta_{i2}(t)$ is equal to 1 when $x_i(t) = 0$ in $I_{i2}(j)$ and is always equal to 0 during $I_{i1}(j)$. Similarly, we denote the total time duration where $\Delta_{i2}(t)$ is equal to 1 in the jth cycle $I_i(j)$ as $T_{e,2}(i,j)$ which is equal to $T_{e,2}(i,j) = \sum_{\ell=1}^{K_2} T_u(i,\ell)$. Thus, we have $\mathbb{E}[T_{e,2}(i)] = \frac{1}{c_i}$. Then, similar to Δ_{i1} in (13), Δ_{i2} is equal to

$$\Delta_{i2} = \frac{\mu_i \lambda_i}{\mu_i + \lambda_i} \frac{s_i}{\mu_i c_i + \lambda_i s_i + c_i s_i}. \tag{15}$$

By using (5), (14), and (15), we obtain Δ_i as

$$\Delta_i = \frac{\mu_i \lambda_i}{\mu_i + \lambda_i} \frac{\theta c_i + (1-\theta)s_i}{\mu_i c_i + \lambda_i s_i + c_i s_i}. \tag{16}$$

Then, by inserting (16) in (7), we obtain Δ. In the next section, we solve the optimization problem in (8).
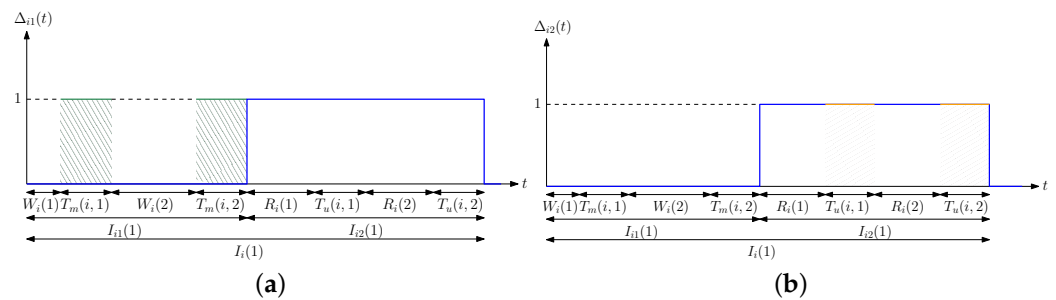

Figure 3. A sample evolution of (**a**) $\Delta_{i1}(t)$, and (**b**) $\Delta_{i2}(t)$ in a typical cycle.

4. Optimization of Average Difference

In this section, we solve the optimization problem in (8). Using Δ_i in (16) in (7), we rewrite (8) as

$$\begin{aligned}
\min_{\{s_i, c_i\}} \quad & \sum_{i=1}^{n} \frac{\mu_i \lambda_i}{\mu_i + \lambda_i} \frac{\theta c_i + (1-\theta)s_i}{\mu_i c_i + \lambda_i s_i + c_i s_i} \\
\text{s.t.} \quad & \sum_{i=1}^{n} s_i + \sum_{i=1}^{n} c_i \leq C \\
& s_i \geq 0, \quad c_i \geq 0, \quad i = 1, \ldots, n.
\end{aligned} \tag{17}$$

We define the Lagrangian function [104] for (17) as

$$\mathcal{L} = \sum_{i=1}^{n} \frac{\mu_i \lambda_i}{\mu_i + \lambda_i} \frac{\theta c_i + (1-\theta)s_i}{\mu_i c_i + \lambda_i s_i + c_i s_i} + \beta \left(\sum_{i=1}^{n} s_i + c_i - C \right) - \sum_{i=1}^{n} \nu_i s_i - \sum_{i=1}^{n} \eta_i c_i, \tag{18}$$

where $\beta \geq 0$, $\nu_i \geq 0$, and $\eta_i \geq 0$. The KKT conditions are

$$\frac{\partial \mathcal{L}}{\partial s_i} = \frac{\mu_i \lambda_i c_i}{\mu_i + \lambda_i} \frac{(1-\theta)\mu_i - \theta(c_i + \lambda_i)}{(\mu_i c_i + \lambda_i s_i + s_i c_i)^2} + \beta - \nu_i = 0, \tag{19}$$

$$\frac{\partial \mathcal{L}}{\partial c_i} = \frac{\mu_i \lambda_i s_i}{\mu_i + \lambda_i} \frac{\theta \lambda_i - (1-\theta)(\mu_i + s_i)}{(\mu_i c_i + \lambda_i s_i + s_i c_i)^2} + \beta - \eta_i = 0, \tag{20}$$

for all i. The complementary slackness conditions are

$$\beta \left(\sum_{i=1}^{n} s_i + c_i - C \right) = 0, \quad \nu_i s_i = 0, \quad \eta_i c_i = 0. \tag{21}$$

First, we find s_i. From (19), we have

$$(\mu_i c_i + \lambda_i s_i + s_i c_i)^2 = \frac{\mu_i \lambda_i c_i}{\mu_i + \lambda_i} \frac{\theta(c_i + \lambda_i) - (1-\theta)\mu_i}{\beta - \nu_i}. \tag{22}$$

When $\theta(c_i + \lambda_i) \geq (1-\theta)\mu_i$, we solve (22) for s_i as

$$s_i = \frac{\mu_i c_i}{\lambda_i + c_i} \left(\sqrt{\frac{1}{\mu_i c_i} \frac{\lambda_i}{\mu_i + \lambda_i} \frac{\theta(c_i + \lambda_i) - (1-\theta)\mu_i}{\beta}} - 1 \right)^+, \tag{23}$$

where we used the fact that we either have $s_i > 0$ and $\nu_i = 0$, or $s_i = 0$ and $\nu_i \geq 0$, due to (21). Here, $(\cdot)^+ = \max(\cdot, 0)$. On the other hand, when $\theta(c_i + \lambda_i) < (1-\theta)\mu_i$, we have $\frac{\partial \Delta_i}{\partial s_i} > 0$, and thus it is optimal to choose $s_i = 0$ as our aim is to minimize Δ in (7). In this case, when $s_i = 0$, we have $\Delta_i = \frac{\theta \lambda_i}{\mu_i + \lambda_i}$ which is independent of the value of c_i. As we obtain the same Δ_i for all values of c_i, and the total update rate is limited, i.e., $\sum_{i=1}^{n} s_i + c_i \leq C$, in this case, it is optimal to choose $c_i = 0$ as well (i.e., when $s_i = 0$).

Next, we find c_i. From (20), we have

$$(\mu_i c_i + \lambda_i s_i + s_i c_i)^2 = \frac{\mu_i \lambda_i s_i}{\mu_i + \lambda_i} \frac{(1-\theta)(\mu_i + s_i) - \theta \lambda_i}{\beta - \eta_i}. \tag{24}$$

When $(1-\theta)(\mu_i + s_i) \geq \theta \lambda_i$, we solve (24) for c_i as

$$c_i = \frac{\lambda_i s_i}{\mu_i + s_i} \left(\sqrt{\frac{1}{\lambda_i s_i} \frac{\mu_i}{\mu_i + \lambda_i} \frac{(1-\theta)(s_i + \mu_i) - \theta \lambda_i}{\beta}} - 1 \right)^+, \tag{25}$$

where we used the fact that we either have $c_i > 0$ and $\eta_i = 0$, or $c_i = 0$ and $\eta_i \geq 0$, due to (21). Similarly, when $(1-\theta)(s_i + \mu_i) < \theta \lambda_i$, we have $\frac{\partial \Delta_i}{\partial c_i} > 0$. Thus, in this case, it is optimal to choose $c_i = 0$. When $c_i = 0$, we have $\Delta_i = \frac{(1-\theta)\mu_i}{\mu_i + \lambda_i}$ which is independent of the value of s_i. Thus, it is optimal to choose $s_i = 0$ when $c_i = 0$.

From (23), if $\frac{1}{\mu_i c_i} \frac{\lambda_i}{\mu_i + \lambda_i} (\theta(c_i + \lambda_i) - (1-\theta)\mu_i) \leq \beta$, we must have $s_i = 0$. Thus, for a given c_i, the optimal test rate allocation policy for s_i is a *threshold policy* where s_i's with small $\frac{1}{\mu_i c_i} \frac{\lambda_i}{\mu_i + \lambda_i} (\theta(c_i + \lambda_i) - (1-\theta)\mu_i)$ are equal to zero. Similarly, from (25), if $\frac{1}{\lambda_i s_i} \frac{\mu_i}{\mu_i + \lambda_i} ((1-\theta)(s_i + \mu_i) - \theta \lambda_i) \leq \beta$, we must have $c_i = 0$. Thus, for a given s_i, the optimal policy to determine c_i is a *threshold policy* where c_i's with small $\frac{1}{\lambda_i s_i} \frac{\mu_i}{\mu_i + \lambda_i} ((1-\theta)(s_i + \mu_i) - \theta \lambda_i)$ are equal to zero.

Next, we show that in the optimal policy, if $s_i > 0$ and $c_i > 0$ for some i, then the total test rate constraint must be satisfied with equality, i.e., $\sum_{i=1}^{n} s_i + c_i = C$.

Lemma 1. *In the optimal policy, if $s_i > 0$ and $c_i > 0$ for some i, then we have $\sum_{i=1}^{n} s_i + c_i = C$.*

Proof of Lemma 1. The derivatives of Δ_i with respect to s_i and c_i are

$$\frac{\partial \Delta_i}{\partial s_i} = \frac{\mu_i \lambda_i c_i}{\mu_i + \lambda_i} \frac{(1 - \theta)\mu_i - \theta(c_i + \lambda_i)}{(c_i \mu_i + s_i c_i + \lambda_i s_i)^2}, \tag{26}$$

$$\frac{\partial \Delta_i}{\partial c_i} = \frac{\mu_i \lambda_i s_i}{\mu_i + \lambda_i} \frac{\theta \lambda_i - (1 - \theta)(s_i + \mu_i)}{(c_i \mu_i + s_i c_i + \lambda_i s_i)^2}. \tag{27}$$

We note that $s_i > 0$ in (23) implies that $\theta(c_i + \lambda_i) > (1 - \theta)\mu_i$. In this case, we have $\frac{\partial \Delta_i}{\partial s_i} < 0$. Similarly, $c_i > 0$ in (25) implies that $(1 - \theta)(s_i + \mu_i) > \theta \lambda_i$. Thus, we have $\frac{\partial \Delta_i}{\partial c_i} < 0$. Therefore, in the optimal policy, if we have $s_i > 0$ and $c_i > 0$ for some i, then we must have $\sum_{i=1}^{n} s_i + c_i = C$. Otherwise, we can further decrease Δ in (7) by increasing c_i or s_i. $\quad\square$

Next, we propose an alternating minimization-based algorithm for finding s_i and c_i. For this purpose, for given initial (s_i, c_i) pairs, we define ϕ_i as

$$\phi_i = \begin{cases} \frac{1}{\mu_i c_i} \frac{\lambda_i}{\mu_i + \lambda_i} (\theta(c_i + \lambda_i) - (1 - \theta)\mu_i), & i = 1, \ldots, n, \\ \frac{1}{\lambda_i s_i} \frac{\mu_i}{\mu_i + \lambda_i} ((1 - \theta)(s_i + \mu_i) - \theta\lambda_i), & i = n + 1, \ldots, 2n. \end{cases} \tag{28}$$

Then, we define u_i as

$$u_i = \begin{cases} \frac{\mu_i c_i}{\lambda_i + c_i} \left(\sqrt{\frac{\phi_i}{\beta}} - 1 \right)^+, & i = 1, \ldots, n, \\ \frac{\lambda_i s_i}{\mu_i + s_i} \left(\sqrt{\frac{\phi_i}{\beta}} - 1 \right)^+, & i = n + 1, \ldots, 2n. \end{cases} \tag{29}$$

From (23) and (25), $s_i = u_i$ and $c_i = u_{n+i}$, for $i = 1, \ldots, n$.

Next, we find s_i and c_i by determining β in (29). First, assume that, in the optimal policy, there is an i such that $s_i > 0$ and $c_i > 0$. Thus, by Lemma 1, we must have $\sum_{i=1}^{n} s_i + c_i = C$. We initially take random (s_i, c_i) pairs such that $\sum_{i=1}^{n} s_i + c_i = C$. Then, given the initial (s_i, c_i) pairs, we immediately choose $u_i = 0$ for $\phi_i < 0$. For the remaining u_i with $\phi_i \geq 0$, we apply a solution method similar to that in [80]. By assuming $\phi_i \geq \beta$, i.e., by disregarding $(\cdot)^+$ in (29), we solve $\sum_{i=1}^{2n} u_i = C$ for β. Then, we compare the smallest ϕ_i which is larger than zero in (28) with β. If we have $\phi_i \geq \beta$, then it implies that $u_i \geq 0$ for all remaining i. Thus, we have obtained u_i values for given initial (s_i, c_i) pairs. If the smallest ϕ_i which is larger than zero is smaller than β, then the corresponding u_i is negative and we should choose $u_i = 0$ for the smallest non-negative ϕ_i. Then, we repeat this procedure until the smallest non-negative ϕ_i is larger than β. After determining all u_i, we obtain $s_i = u_i$ and $c_i = u_{n+i}$ for $i = 1, \ldots, n$. Then, with the updated values of (s_i, c_i) pairs, we keep finding u_i's until the KKT conditions in (19) and (20) are satisfied.

We note that for indices (persons) i for which (s_i, c_i) are zero, the health care provider does not perform any tests, and maps these people as either always infected, i.e., $\hat{x}_i(t) = 1$ for all t, or always healthy, i.e., $\hat{x}_i(t) = 0$. If $\hat{x}_i(t) = 0$ for all t, $\Delta_i = \frac{\theta\lambda_i}{\mu_i + \lambda_i}$, and if $\hat{x}_i(t) = 1$ for all t, $\Delta_i = \frac{(1-\theta)\mu_i}{\mu_i + \lambda_i}$. Thus, for such i, the health care provider should choose $\hat{x}_i(t) = 0$ for all t, if $\frac{\theta\lambda_i}{\mu_i + \lambda_i} < \frac{(1-\theta)\mu_i}{\mu_i + \lambda_i}$, and should choose $\hat{x}_i(t) = 1$ for all t, otherwise, without performing any tests.

Finally, we note that the problem in (17) is not a convex optimization problem as the objective function is not jointly convex in s_i and c_i. Therefore, the solutions obtained via the proposed method may not be globally optimal. For this reason, we select different initial starting points and apply the proposed alternating minimization-based algorithm and choose the solution that achieves the smallest Δ in (7).

In the next section, we first provide an alternative method to find the average difference Δ in (6) and then characterize the average difference for the erroneous test measurements.

5. Average Difference for the Case with Erroneous Test Measurements

We note that the infection status of the ith person and its estimate at the health care provider form a continuous time Markov chain (Section 7.5 of [105]) with the states $(x_i(t), \hat{x}_i(t)) \in \{(0,0), (0,1), (1,0), (1,1)\}$. In this section, by finding the steady-state distribution for $(x_i(t), \hat{x}_i(t))$, we provide an alternative method to find Δ in (6). Then, we consider the case with erroneous test measurements. For this case, we characterize the long-term average difference for the ith person denoted by Δ_i^e.

5.1. An Alternative Method to Characterize Average Difference

When there is no error in the tests, the state transition graph is shown in Figure 4a. Assuming that $s_i > 0$, $c_i > 0$, every state is accessible from any other state, and thus, the Markov chain induced by the system is irreducible. Note that in Section 4, we see that the testing rates for some people can be equal to 0, i.e., $s_i = 0$ and $c_i = 0$. For these people, we choose $\hat{x}_i(t)$ to be either always 0 or 1, i.e., consider them as always healthy or sick all the time. Depending on the choice of $\hat{x}_i(t)$, when $s_i = 0$ and $c_i = 0$, either the states $(0,0)$ and $(1,0)$, or the states $(0,1)$ and $(1,1)$ will be transient, and thus, have 0 probability in the steady state. By using small time-step approximation to a discrete time Markov chain, one can show that the self transition probabilities are non-zero, and thus, the Markov chain induced by the system is also aperiodic (Section 7.5 of [105]). Therefore, the Markov chain shown in Figure 4a admits a unique stationary distribution given by $\boldsymbol{\pi} = \{\pi_{00}, \pi_{01}, \pi_{10}, \pi_{11}\}$. We find the stationary distribution by writing the local-balance equations which are given as

$$\pi_{00}\lambda_i = \pi_{10}\mu_i + \pi_{01}c_i, \tag{30}$$
$$\pi_{10}(\mu_i + s_i) = \pi_{00}\lambda_i, \tag{31}$$
$$\pi_{01}(c_i + \lambda_i) = \pi_{11}\mu_i, \tag{32}$$
$$\pi_{11}\mu_i = \pi_{10}s_i + \pi_{01}\lambda_i. \tag{33}$$

By using (30)–(33) and $\sum_{k=1}^{2}\sum_{\ell=1}^{2}\pi_{k\ell} = 1$, we find the steady-state distribution $\boldsymbol{\pi}$ as

$$\pi_{01} = \frac{\mu_i\lambda_i}{\mu_i + \lambda_i}\frac{s_i}{\mu_i c_i + \lambda_i s_i + c_i s_i}, \tag{34}$$

$$\pi_{10} = \frac{\mu_i\lambda_i}{\mu_i + \lambda_i}\frac{c_i}{\mu_i c_i + \lambda_i s_i + c_i s_i}, \tag{35}$$

and $\pi_{00} = \frac{\mu_i + s_i}{\lambda_i}\pi_{10}$, and $\pi_{11} = \frac{c_i + \lambda_i}{\mu_i}\pi_{01}$. We note that Δ_{i1} in (14) is also equal to π_{10} in (35), i.e., we have $\Delta_{i1} = \pi_{10}$. Similarly, Δ_{i2} in (15) is equal to π_{01} in (34). Thus, by observing that the states $(x_i(t), \hat{x}_i(t))$ form a continuous time Markov chain, we can find the average difference Δ in (6) by finding the steady-state distribution for $\boldsymbol{\pi}$. This method will be particularly useful in the following section where we consider the case with erroneous test measurements.
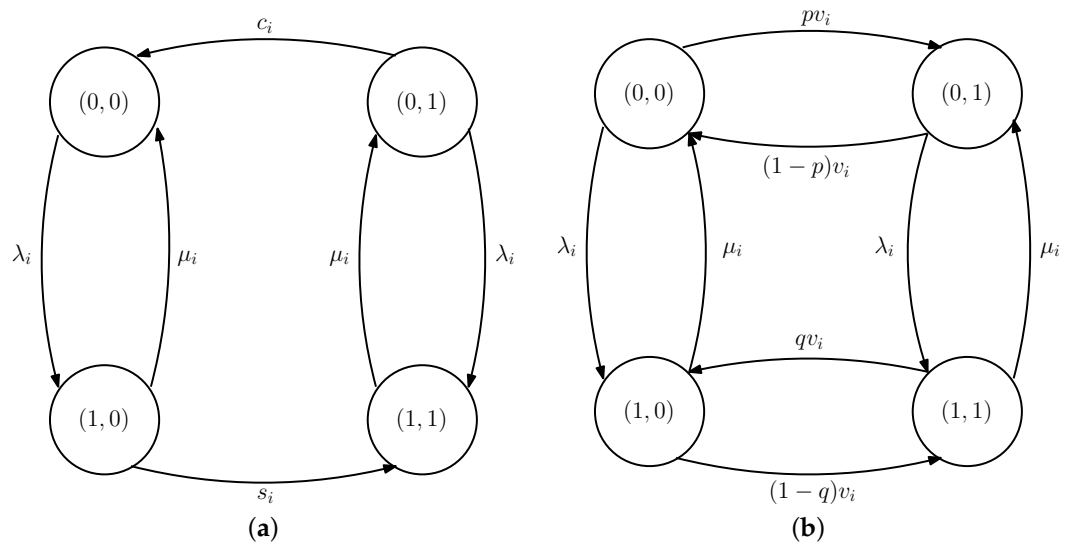
Figure 4. Transition graphs of the states $(x_i(t), \hat{x}_i(t))$ (**a**) when there is no error in the tests, and (**b**) when there are errors in the tests.

5.2. Average Difference with Erroneous Test Measurements

In this section, we consider the case where the test measurements can be erroneous. When a test in applied to an infected person, i.e., when $x_i(t) = 1$, the test result will be 0 with probability q and 1 with probability $1 - q$, where $0 \le q < \frac{1}{2}$. In other words, the false-negative probability is equal to q. Similarly, when a test is applied to a healthy person, i.e., when $x_i(t) = 0$, the test result will be 1 with probability p and 0 with probability $1 - p$, where $0 \le p < \frac{1}{2}$. Thus, the false-positive probability is equal to p. The probability distribution for the test measurements is provided in Table 2.

Table 2. The probability distribution for successful and false test measurements.

$x_i(t) \setminus \hat{x}_i(t)$	**0**	**1**
0	$1 - p$	p
1	q	$1 - q$

In this section, we consider the case where the health care provider applies only one test rate v_i to the ith person, whether the person is currently marked as healthy or infected. That is, we do not consider separate testing rates of s_i and c_i for healthy and infected people as we did before, instead, here both s_i and c_i are equal o v_i. Since the health care provider applies the same test rate for the ith person, here we do not consider the importance factor θ either. Then, we define the long-term average difference for the ith person with the error on the test measurements as follows, where the superscript e stands for "erroneous".

$$\Delta_i^e = \Delta_{i1}^e + \Delta_{i2}^e, \tag{36}$$

and the definitions of Δ_{i1}^e and Δ_{i2}^e follow similarly from (13). We note that with the test rates v_i and errors on the test measurements, the states $(x_i(t), \hat{x}_i(t))$ form a continuous time Markov chain, and the corresponding state transition graph is shown in Figure 4b. Assuming that $v_i > 0$, one can show that there is a unique steady-state distribution $\boldsymbol{\pi}^e = \{\pi_{00}^e, \pi_{01}^e, \pi_{10}^e, \pi_{11}^e\}$ which can be found by solving the local balance equations which are given as follows

$$\pi_{00}^e(v_i p + \lambda_i) = \pi_{01}^e v_i(1-p) + \pi_{10}^e \mu_i, \tag{37}$$

$$\pi_{10}^e(v_i(1-q) + \mu_i) = \pi_{00}^e \lambda_i + \pi_{11}^e v_i q, \tag{38}$$

$$\pi_{01}^e(v_i(1-p) + \lambda_i) = \pi_{00}^e v_i p + \pi_{11}^e \mu_i, \tag{39}$$

$$\pi_{11}^e(v_i q + \mu_i) = \pi_{10}^e v_i(1-q) + \pi_{01}^e \lambda_i. \tag{40}$$

Then, by using (37)–(40) and $\sum_{k=1}^{2} \sum_{\ell=1}^{2} \pi_{k\ell}^e = 1$, we find the steady-state distribution $\boldsymbol{\pi}^e$ as

$$\pi_{00}^e = \frac{\mu_i \lambda_i q + (1-p)\mu_i(v_i + \mu_i)}{(\lambda_i + \mu_i)(\lambda_i + \mu_i + v_i)}, \tag{41}$$

$$\pi_{01}^e = \frac{\mu_i \lambda_i(1-q) + p\mu_i(v_i + \mu_i)}{(\lambda_i + \mu_i)(\lambda_i + \mu_i + v_i)}, \tag{42}$$

$$\pi_{10}^e = \frac{\mu_i \lambda_i(1-p) + q\lambda_i(v_i + \lambda_i)}{(\lambda_i + \mu_i)(\lambda_i + \mu_i + v_i)}, \tag{43}$$

$$\pi_{11}^e = \frac{\mu_i \lambda_i p + (1-q)\lambda_i(v_i + \lambda_i)}{(\lambda_i + \mu_i)(\lambda_i + \mu_i + v_i)}. \tag{44}$$

We note that Δ_{i1}^e, and Δ_{i2}^e are equal to π_{10}^e in (43), and π_{01}^e in (42), respectively. Thus, if $v_i > 0$, then Δ_i^e in (36) becomes

$$\Delta_i^e = \frac{p\mu_i^2 + q\lambda_i^2 + (2 - p - q)\mu_i\lambda_i + v_i(p\mu_i + q\lambda_i)}{(\lambda_i + \mu_i)(\lambda_i + \mu_i + v_i)}. \tag{45}$$

We immediately note that if false-positive test probability p and false-negative test probability q are equal to 0, Δ_i^e becomes $\frac{2\mu_i\lambda_i}{(\lambda_i+\mu_i)(\lambda_i+\mu_i+v_i)}$ which is equal to $\Delta_{i1} + \Delta_{i2}$ provided in (14) and (15), respectively, when $v_i = s_i = c_i$. Then, $\frac{\partial \Delta_i^e}{\partial p} \geq 0$ is equivalent to $v_i + \mu_i - \lambda_i \geq 0$ and $\frac{\partial \Delta_i^e}{\partial q} \geq 0$ is equivalent to $v_i + \lambda_i - \mu_i \geq 0$ which means that depending on the values of v_i, μ_i, and λ_i, the long-term average difference Δ_i^e can be an increasing function of only p or only q, or both p and q, but Δ_i^e cannot be a decreasing function of both p and q. This is expected as false-negative and false-positive tests negatively affect the estimation process. One can also show that $\frac{\partial \Delta_i^e}{\partial v_i} < 0$ and $\frac{\partial^2 \Delta_i^e}{\partial v_i^2} > 0$ which means that Δ_i^e decreases with v_i and is a convex function of the test rate v_i.

Next, we consider the case when $v_i = 0$. Note that when $v_i = 0$, the health care provider either maps these people as always sick or always healthy depending on their infection and recovery rates. Thus, when $v_i = 0$ and depending on the estimate $\hat{x}_i(t)$, two of the states in Figure 4b will never be visited and thus, these states will have 0 steady-state probabilities. For this case, the steady states are given by $\bar{\pi}_{1,\hat{x}_i}^e$ and $\bar{\pi}_{0,\hat{x}_i}^e$. The local balance equation is $\lambda_i \bar{\pi}_{0,\hat{x}_i}^e = \mu_i \bar{\pi}_{1,\hat{x}_i}^e$. By using $\bar{\pi}_{0,\hat{x}_i}^e + \bar{\pi}_{1,\hat{x}_i}^e = 1$, we find the steady-state distribution as $\bar{\pi}_{0,\hat{x}_i}^e = \frac{\mu_i}{\mu_i + \lambda_i}$, and $\bar{\pi}_{1,\hat{x}_i}^e = \frac{\lambda_i}{\mu_i + \lambda_i}$. Thus, if $\mu_i < \lambda_i$, i.e., if people are infected more frequently, then the health care provider chooses its estimate as $\hat{x}_i(t) = 1$ and, $\Delta_i^e = \frac{\mu_i}{\mu_i + \lambda_i}$. If $\mu_i \geq \lambda_i$, i.e., if people stay healthy more often, then we have $\hat{x}_i(t) = 0$, and $\Delta_i^e = \frac{\lambda_i}{\mu_i + \lambda_i}$. Therefore, when $v_i = 0$, we have

$$\Delta_i^e = \min\left\{ \frac{\mu_i}{\mu_i + \lambda_i}, \frac{\lambda_i}{\mu_i + \lambda_i} \right\}. \tag{46}$$

In order to find the optimal test rates v_i in the case of errors on the test measurements, we formulate the following optimization problem

$$\min_{\{v_i\}} \quad \sum_{i=1}^{n} \mathbb{1}\{v_i > 0\} \frac{p\mu_i^2 + q\lambda_i^2 + (2 - p - q)\mu_i\lambda_i + v_i(p\mu_i + q\lambda_i)}{(\lambda_i + \mu_i)(\lambda_i + \mu_i + v_i)}$$

$$+ \mathbb{1}\{v_i = 0\} \min\left\{\frac{\mu_i}{\mu_i + \lambda_i}, \frac{\lambda_i}{\mu_i + \lambda_i}\right\}$$

$$\text{s.t.} \quad \sum_{i=1}^{n} v_i \leq C$$

$$v_i \geq 0, \quad i = 1, \ldots, n, \tag{47}$$

where the objective function is given by the summation of Δ_i^e in (45) when $v_i > 0$ and Δ_i^e in (46) when $v_i = 0$ over all people and $\mathbb{1}\{.\}$ is the indicator function taking value 1 when $\{\cdot\}$ is true and 0, otherwise. In (47), we have a constraint on the total test rate, i.e., $\sum_{i=1}^{n} v_i \leq C$. We note that the optimization problem in (47) is in general not convex due to the indicator function in the objective function. However, for a given set of $\mathbb{1}\{v_i = 0\}$, the optimization problem in (47) is convex and can be solved optimally. Thus, by solving the problem in (47) for all possible set of $\mathbb{1}\{v_i = 0\}$, we can determine the global optimal solution which requires to solve 2^n different optimization problems which can be impractical for large n. Because of this reason, next, we provide a greedy algorithm to solve the optimization problem in (47).

In the greedy solution, initially, assuming that $\mathbb{1}\{v_i > 0\} = 1$ for all i, we consider the following the optimization problem

$$\min_{\{v_i\}} \quad \sum_{i=1}^{n} \frac{p\mu_i^2 + q\lambda_i^2 + (2 - p - q)\mu_i\lambda_i + v_i(p\mu_i + q\lambda_i)}{(\lambda_i + \mu_i)(\lambda_i + \mu_i + v_i)}$$

$$\text{s.t.} \quad \sum_{i=1}^{n} v_i \leq C$$

$$v_i \geq 0, \quad i = 1, \ldots, n, \tag{48}$$

where the objective function in (48) is equal to Δ_i^e in (45). For this optimization problem, we define the Lagrangian function for (48) as

$$\mathcal{L} = \sum_{i=1}^{n} \frac{p\mu_i^2 + q\lambda_i^2 + (2 - p - q)\mu_i\lambda_i + v_i(p\mu_i + q\lambda_i)}{(\lambda_i + \mu_i)(\lambda_i + \mu_i + v_i)} + \bar{\beta}\left(\sum_{i=1}^{n} v_i - C\right) - \sum_{i=1}^{n} \bar{v}_i v_i, \tag{49}$$

where $\bar{\beta} \geq 0$, $\bar{v}_i \geq 0$. We note that the problem defined in (48) is a convex optimization problem, and thus we can find the optimal test rates v_i by analyzing the KKT and the complementary slackness conditions. The KKT conditions are given by

$$\frac{\partial \mathcal{L}}{\partial v_i} = \frac{-2(1 - p - q)\mu_i\lambda_i}{(\mu_i + \lambda_i)(\mu_i + \lambda_i + v_i)^2} + \bar{\beta} - \bar{v}_i = 0, \tag{50}$$

for all i. The complementary slackness conditions are

$$\bar{\beta}\left(\sum_{i=1}^{n} v_i - C\right) = 0, \quad \bar{v}_i v_i = 0. \tag{51}$$

By using (50) and (51), we find the optimal v_i values for the problem in (48) as

$$v_i = (\mu_i + \lambda_i)\left(\sqrt{\frac{\mu_i\lambda_i}{(\mu_i + \lambda_i)^3} \frac{2(1 - p - q)}{\bar{\beta}}} - 1\right)^+. \tag{52}$$

With the test rates v_i in (52) we find the average differences Δ_i^e in (45) and then compare them with Δ_i^e in (46) when $v_i = 0$. Due to the errors in the tests, Δ_i^e in (46) with $v_i = 0$ can be smaller than Δ_i^e in (45) with the test rates v_i found in (52). For these people, we

choose index i where the difference between Δ_i^e in (45) with the v_i in (52) and Δ_i^e in (46) is the highest. Then, we take $v_i = 0$ as applying no test to this person can further decrease Δ_i^e. For the remaining people, we solve the optimization problem in (48). After obtaining the test rates for the remaining people, we again compare average differences Δ_i^e with the test rates in (52) and with no test and we choose $v_i = 0$ for the person where Δ_i^e can be further decreased. We repeat these steps until all Δ_i^es with $v_i > 0$ cannot be further decreased by choosing $v_i = 0$.

We note that the solution obtained in (52) has a *threshold* structure. As false-positive and -negative test rates increase, the term $\frac{2(1-p-q)}{\bar{\beta}}$ in (52) becomes smaller. As a result, some people with higher $\sqrt{\frac{(\mu_i+\lambda_i)^3}{\mu_i\lambda_i}}$ may not be tested by the health care provider. Thus, when p and q are high, a smaller portion of the population is tested with higher test rates in order to combat the test errors.

6. Average Estimation Error with Dependent Infection Rates

In this section, we consider the case where we have two people whose infection rates depend on each other. When these two people are healthy, they can be individually infected with the virus after an exponential time with rate λ. When one of these two people is infected and this has not been detected by the health care provider, this person can infect the other healthy person after an exponential time with rate λ_{12} which has been illustrated in Figure 5. Thus, when both of the people are healthy, their individual infection rate is λ. However, when one of them is sick and this has not been detected by the health care provider, the healthy person's total infection rate is equal to $\lambda + \lambda_{12}$. On the other hand, if only one person is infected, i.e., $x_i(t) = 1$, which has also been detected by the health care provider, $\hat{x}_i(t) = 1$, then we assume that we isolate the infected person from the healthy one, and thus, the healthy person's infection rate remains as λ instead of $\lambda + \lambda_{12}$. When the people are infected, they recover from the disease after an exponential time with rate μ.
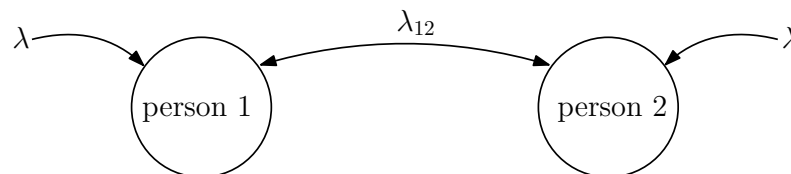

Figure 5. The infection rates of two people where the individual infection rate is equal to λ. When the infection has not been detected, these two people can infect each other with rate λ_{12}.

When the health care provider believes that a person is healthy, i.e., $\hat{x}_i(t) = 0$, the next test is applied to this person after an exponential time with rate s. When the health care provider believes that a person is sick, i.e., $\hat{x}_i(t) = 1$, the next test applied to this person after an exponential time with rate c. Here, we note that since the people are identical in terms of their infection and recovery rates, the health care provider applies the same test rates.

Similar to Section 5, we note that the states $\{x_1(t), \hat{x}_1(t), x_2(t), \hat{x}_2(t)\}$ form a continuous time Markov chain where the unique stationary distribution is given by $\boldsymbol{\pi}^d = \{\pi_{0000}^d, \pi_{0001}^d, \ldots, \pi_{1111}^d\}$. In order to find the stationary distribution, we write the local balance equations as follows

$$2\lambda \pi_{0000}^d = \mu \pi_{1000}^d + c\pi_{0100}^d + \mu \pi_{0010}^d + c\pi_{0001}^d, \tag{53}$$

$$(2\lambda + c)\pi_{0001}^d = \mu \pi_{0011}^d + c\pi_{0101}^d + \mu \pi_{1001}^d, \tag{54}$$

$$(\lambda + \lambda_{12} + \mu + s)\pi_{0010}^d = c\pi_{0110}^d + \mu \pi_{1010}^d + \lambda \pi_{0000}^d, \tag{55}$$

$$(\lambda + \mu)\pi_{0011}^d = c\pi_{0111}^d + \mu \pi_{1011}^d + s\pi_{0010}^d + \lambda \pi_{0001}^d, \tag{56}$$

$$(2\lambda + c)\pi_{0100}^d = c\pi_{0101}^d + \mu\pi_{0110}^d + \mu\pi_{1100}^d, \tag{57}$$

$$(2\lambda + 2c)\pi_{0101}^d = \mu\pi_{0111}^d + \mu\pi_{1101}^d, \tag{58}$$

$$(\lambda + \mu + s + c)\pi_{0110}^d = \lambda\pi_{0100}^d + \mu\pi_{1110}^d, \tag{59}$$

$$(\lambda + \mu + c)\pi_{0111}^d = s\pi_{0110}^d + \lambda\pi_{0101}^d + \mu\pi_{1111}^d, \tag{60}$$

$$(\lambda + \lambda_{12} + \mu + s)\pi_{1000}^d = \lambda\pi_{0000}^d + c\pi_{1001}^d + \mu\pi_{1010}^d, \tag{61}$$

$$(\lambda + \mu + s + c)\pi_{1001}^d = \mu\pi_{1011}^d + \lambda\pi_{0001}^d, \tag{62}$$

$$(2\mu + 2s)\pi_{1010}^d = (\lambda + \lambda_{12})\pi_{1000}^d + (\lambda + \lambda_{12})\pi_{0010}^d, \tag{63}$$

$$(2\mu + s)\pi_{1011}^d = s\pi_{1010}^d + \lambda\pi_{1001}^d + \lambda\pi_{0011}^d, \tag{64}$$

$$(\lambda + \mu)\pi_{1100}^d = s\pi_{1000}^d + \lambda\pi_{0100}^d + c\pi_{1101}^d + \mu\pi_{1110}^d, \tag{65}$$

$$(\lambda + \mu + c)\pi_{1101}^d = s\pi_{1001}^d + \lambda\pi_{0101}^d + \mu\pi_{1111}^d, \tag{66}$$

$$(2\mu + s)\pi_{1110}^d = \lambda\pi_{1100}^d + s\pi_{1010}^d + \lambda\pi_{0110}^d, \tag{67}$$

$$2\mu\pi_{1111}^d = s\pi_{1110}^d + \lambda\pi_{1101}^d + s\pi_{1011}^d + \lambda\pi_{0111}^d. \tag{68}$$

By using (53)–(68) and $\sum_{j=1}^2 \sum_{\ell=1}^2 \sum_{m=1}^2 \sum_{h=1}^2 \pi_{j\ell mh}^d = 1$, we find the stationary distribution $\boldsymbol{\pi}^d$. We denote the long-term average estimation error for person i as Δ_i^d for $i = 1, 2$, where the superscript d stands for "dependent", which is given by

$$\Delta_i^d = \Delta_{i1}^d + \Delta_{i2}^d, \tag{69}$$

where Δ_{i1}^d and Δ_{i2}^d follow from (13). Then, we have

$$\Delta_{11}^d = \pi_{1000}^d + \pi_{1001}^d + \pi_{1010}^d + \pi_{1011}^d, \tag{70}$$

$$\Delta_{12}^d = \pi_{0100}^d + \pi_{0101}^d + \pi_{0110}^d + \pi_{0111}^d, \tag{71}$$

$$\Delta_{21}^d = \pi_{0010}^d + \pi_{0110}^d + \pi_{1010}^d + \pi_{1110}^d, \tag{72}$$

$$\Delta_{22}^d = \pi_{0001}^d + \pi_{0101}^d + \pi_{1001}^d + \pi_{1101}^d. \tag{73}$$

In Section 8, for given infection, recovery and test rates, we numerically evaluate the stationary distribution and find the average difference Δ_i^d.

7. Age of Incorrect Information Based Error Metric

To date, we have considered an estimation error metric that takes the value 1 if the actual infection status of a person is different than the real-time estimation at the health care provider. Thus, the error metric takes values based on the information content. On the other hand, the traditional age metric introduced in [1] considers only the time passed since the most recently received status update packet is generated at the source. As a result, the traditional age metric does not consider the information content and age alone may not be a suitable performance metric for the problem considered in our work.

In the context of infection tracking, it is important to know how long the estimations at the health care provider have been different from the actual infection status of the people. However, the error metric that we have considered thus far does not have the time component, i.e., it only takes value 1 independent of the time duration that it has been off from the actual health status. Motivated by the AoII introduced in [51,102] which accounts for both the time and the information content, in this section, we consider the following error metric, where the superscript s stands for "synchronization" implied in AoII,

$$\Delta_i^s = (t - V_i(t))\mathbb{1}\{\hat{x}_i(t) \neq x_i(t)\}, \tag{74}$$

where $V_i(t)$ is the last time instant where the health care provider makes an accurate estimation of the health status for the ith person, i.e., the last time instant when $\Delta_i^s = 0$. Similarly, we define

$$\Delta_{i1}^s = (t - V_{i1}(t)) \max\{x_i(t) - \hat{x}_i(t), 0\}, \tag{75}$$

$$\Delta_{i2}^s = (t - V_{i2}(t)) \max\{\hat{x}_i(t) - x_i(t), 0\}, \tag{76}$$

where $V_{i1}(t)$ and $V_{i2}(t)$ are equal to the last time instants when Δ_{i1}^s and Δ_{i2}^s are equal to 0, respectively. A sample evolution of Δ_{i1}^s and Δ_{i2}^s is shown in Figure 6 and we note that $\Delta_i^s(t) = \Delta_{i1}^s(t) + \Delta_{i2}^s(t)$.
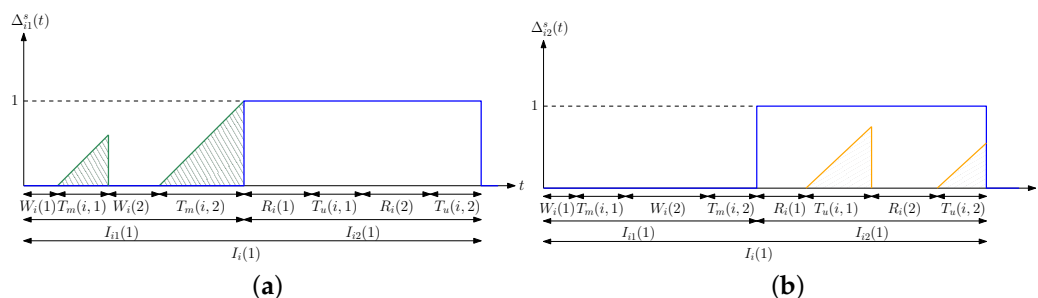

Figure 6. A sample evolution of (**a**) $\Delta_{i1}^s(t)$, and (**b**) $\Delta_{i2}^s(t)$ in a typical update cycle.

Similar to Section 3, the infection and the recovery rates of the ith person are λ_i and μ_i, respectively. In this section, the health care provider applies only one test rate for each person denoted by w_i. That is, we do not consider separate testing rates of s_i and c_i for healthy and infected people as we did previously, instead, here both s_i and c_i are equal o w_i. We first consider the case where $w_i > 0$. By following the steps in Section 3, one can show that $\mathbb{E}[I_{i1}] = \frac{1}{w_i} + \frac{w_i + \mu_i}{w_i \lambda_i}$ and $\mathbb{E}[I_{i2}] = \frac{1}{w_i} + \frac{w_i + \lambda_i}{w_i \mu_i}$ which can be obtained by substituting w_i instead of s_i and c_i in (10) and (12), respectively. Next, we denote the total area when $\Delta_{i1}^s(t) > 0$ as $A_{e,1}(i,j)$ during the jth cycle where $A_{e,1}(i,j) = \sum_{\ell=1}^{K_1} \frac{T_m(i,\ell)^2}{2}$ and K_1 has a geometric distribution with success rate $\frac{w_i}{\mu_i + w_i}$. Then, we have $\mathbb{E}[A_{e,1}(i)] = \frac{1}{w_i(w_i + \mu_i)}$. Similarly, we denote the total area when $\Delta_{i2}^s(t) > 0$ as $A_{e,2}(i,j)$ during the jth cycle where $A_{e,2}(i,j) = \sum_{\ell=1}^{K_2} \frac{T_u(i,\ell)^2}{2}$ and K_2 has a geometric distribution with success rate $\frac{w_i}{\lambda_i + w_i}$. Then, we have $\mathbb{E}[A_{e,2}(i)] = \frac{1}{w_i(w_i + \lambda_i)}$. By using ergodicity, the long-term average differences become $\Delta_{i1}^s = \frac{\mathbb{E}[A_{e,1}(i)]}{\mathbb{E}[I_{i1}] + \mathbb{E}[I_{i2}]}$ and $\Delta_{i2}^s = \frac{\mathbb{E}[A_{e,2}(i)]}{\mathbb{E}[I_{i1}] + \mathbb{E}[I_{i2}]}$ which gives

$$\Delta_i^s = \Delta_{i1}^s + \Delta_{i2}^s = \frac{\mu_i \lambda_i}{\mu_i + \lambda_i} \frac{2w_i + \mu_i + \lambda_i}{(w_i + \mu_i + \lambda_i)(w_i + \mu_i)(w_i + \lambda_i)}, \tag{77}$$

when $w_i > 0$. One can show that Δ_i^s is a decreasing function of w_i, i.e., $\frac{\partial \Delta_i^s}{\partial w_i} < 0$, and Δ_i^s is a convex function of w_i, i.e., $\frac{\partial^2 \Delta_i^s}{\partial w_i^2} > 0$.

When $w_i = 0$, we have $\mathbb{E}[I_i] = \frac{\mu_i \lambda_i}{\mu_i + \lambda_i}$, i.e., $\mathbb{E}[I_i]$ is equal to the expected time of a person's healthy and sick states. Since the health care provider applies no tests to test a person, it either estimates this person to be always sick ($\hat{x}_i(t) = 1$) or always healthy ($\hat{x}_i(t) = 0$). When $w_i = 0$ and $\hat{x}_i(t) = 1$, then $\Delta_i^s = \frac{1}{\mu_i} \frac{\lambda_i}{\mu_i + \lambda_i}$. When $w_i = 0$ and $\hat{x}_i(t) = 1$, we have $\Delta_i^s = \frac{1}{\lambda_i} \frac{\mu_i}{\mu_i + \lambda_i}$. If $\mu_i < \lambda_i$, then the health care provider $\hat{x}_i(t) = 1$, and $\hat{x}_i(t) = 0$, otherwise. Thus, when $w_i = 0$, we have $\Delta_i^s = \min\left\{\frac{1}{\mu_i} \frac{\lambda_i}{\mu_i + \lambda_i}, \frac{1}{\lambda_i} \frac{\mu_i}{\mu_i + \lambda_i}\right\}$.

In order to find the optimal test rates, we formulate the following optimization problem

$$\min_{\{w_i\}} \quad \sum_{i=1}^{n} \mathbb{1}\{w_i > 0\} \frac{\mu_i \lambda_i}{\mu_i + \lambda_i} \frac{2w_i + \mu_i + \lambda_i}{(w_i + \mu_i + \lambda_i)(w_i + \mu_i)(w_i + \lambda_i)}$$

$$+ \mathbb{1}\{w_i = 0\} \min\left\{\frac{1}{\mu_i} \frac{\lambda_i}{\mu_i + \lambda_i}, \frac{1}{\lambda_i} \frac{\mu_i}{\mu_i + \lambda_i}\right\}$$

$$\text{s.t.} \quad \sum_{i=1}^{n} w_i \le C$$

$$w_i \ge 0, \quad i = 1, \dots, n, \tag{78}$$

where the objective function in (78) is equal to the summation of Δ_i^s in (77) when $w_i > 0$ and Δ_i^s when $w_i = 0$ over all people. In order to solve the problem in (78), we follow the same greedy solution approach in Section 5. First, by assuming that $w_i > 0$, and thus, the average difference Δ_i^s is given in (77), we solve the following optimization problem

$$\min_{\{w_i\}} \quad \sum_{i=1}^{n} \frac{\mu_i \lambda_i}{\mu_i + \lambda_i} \frac{2w_i + \mu_i + \lambda_i}{(w_i + \mu_i + \lambda_i)(w_i + \mu_i)(w_i + \lambda_i)}$$

$$\text{s.t.} \quad \sum_{i=1}^{n} w_i \le C$$

$$w_i \ge 0, \quad i = 1, \dots, n. \tag{79}$$

Since the problem in (79) is a convex optimization problem, by defining Lagrangian function and analyzing the KKT and the complementary slackness conditions, we can find the optimal w_i values. In order to avoid being repetitive, we skip these optimization steps. Then, we compare Δ_i^s in (77) with w_i values found in (79) with $\min\{\frac{1}{\mu_i} \frac{\lambda_i}{\mu_i + \lambda_i}, \frac{1}{\lambda_i} \frac{\mu_i}{\mu_i + \lambda_i}\}$. If we can reduce Δ_i^s further, we choose $w_i = 0$ for the person with the highest improvement. Then, we solve the optimization problem in (79) for the remaining people. We repeat these steps until there is no improvement in Δ_i^s by choosing $w_i = 0$.

In the next section, we provide extensive numerical results to evaluate optimal test rates in various settings considered in this paper.

8. Numerical Results

In this section, we provide seven numerical results. For these examples, we take λ_i as

$$\lambda_i = ar^i, \quad i = 1, \dots, n, \tag{80}$$

where $r = 0.9$ and a is such that $\sum_{i=1}^{n} \lambda_i = 6$. Furthermore, we take μ_i as

$$\mu_i = bq^i, \quad i = 1, \dots, n, \tag{81}$$

where $q = 1.1$ and b is such that $\sum_{i=1}^{n} \mu_i = 4$. Since λ_i in (80) decreases with i, people with lower indices become infected more quickly compared to people with higher indices. Since μ_i in (81) increases with i, people with higher indices recover more quickly compared to people with lower indices. Thus, a person with a low index becomes infected quickly and recovers slowly.

In the first example, we take the total number of people as $n = 10$, the total test rate as $C = 16$, and $\theta = 0.5$. We start with randomly chosen s_i and c_i such that $\sum_{i=1}^{n} s_i + c_i = 16$, and apply the alternating minimization-based method proposed in Section 4. We repeat this process for 30 different initial (s_i, c_i) pairs and choose the solution that gives the smallest Δ. In Figure 7a, we observe that the first three people are never tested by the health care provider. We note that s_i, which is the test rate when $\hat{x}_i(t) = 0$, initially increases with i but then decreases with i. This means that people who become infected rarely are tested less frequently when they are marked as healthy. Similarly, we observe in Figure 7a that

c_i, which is the test rate when $\hat{x}_i(t) = 1$, monotonically increases with i. In other words, people who recover from the virus quickly are tested more frequently when they are marked as infected.
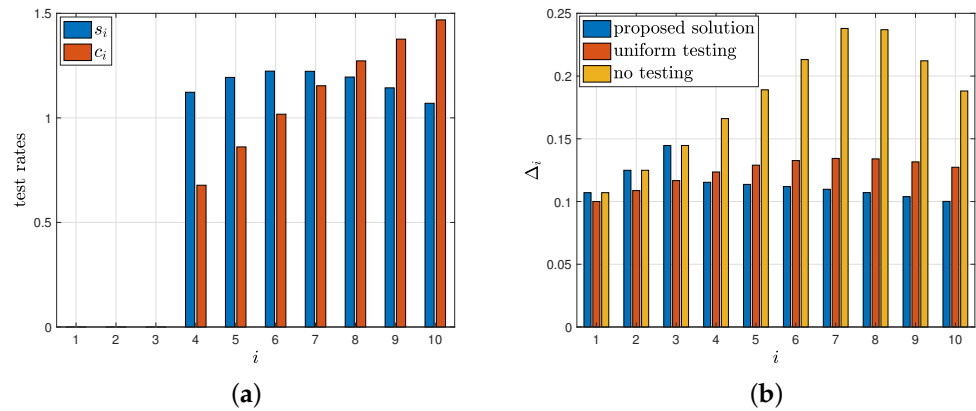

Figure 7. (**a**) Test rates s_i and c_i, (**b**) corresponding average difference Δ_i.

In Figure 7b, we plot Δ_i resulting from the solution found from the proposed algorithm, Δ_i when the health care provider applies tests to everyone in the population uniformly, i.e., $s_i = c_i = \frac{C}{2n}$ for all i, and Δ_i when the health care provider applies no tests, i.e., $s_i = c_i = 0$ for all i. In the case of no tests, we have $\Delta_i = \min\{\frac{\theta\lambda_i}{\mu_i+\lambda_i}, \frac{(1-\theta)\mu_i}{\mu_i+\lambda_i}\}$. We observe in Figure 7b that the health care provider applies tests on people whose Δ_i can be reduced the most as opposed to uniform testing where everyone is tested equally. Thus, the first three people who have the smallest Δ_i are not tested by the health care provider. With the proposed solution, by not testing the first three people, Δ_i are further reduced for the remaining people compared to uniform testing. For the people who are not tested, the health care provider chooses $\hat{x}_i(t) = 1$ all the time, i.e., marks these people always sick as $\frac{\theta\lambda_i}{\mu_i+\lambda_i} > \frac{(1-\theta)\mu_i}{\mu_i+\lambda_i}$. This is expected as these people have high λ_i and low μ_i, i.e., they are infected easily and they stay sick for a long time.

In the second example, we use the same set of variables except for the total test rate C. We vary the total test rate C in between 5 and 20. We plot Δ with respect to C in Figure 8. We observe that Δ decreases with C. Thus, with higher total test rates, the health care provider can track the infection status of the population better as expected.

In the third example, we use the same set of variables except for the total number of people n. In addition, we also use uniform infection and healing rates, i.e., $\lambda_i = \frac{6}{n}$ and $\mu_i = \frac{4}{n}$ for all i, for comparison with λ_i in (80) and μ_i in (81), while keeping the total infection and healing rates the same, i.e., $\sum_{i=1}^{n} \lambda_i = 6$ and $\sum_{i=1}^{n} \mu_i = 4$, for both cases. We vary the number of people n from 2 to 30. We observe in Figure 9 that when the infection and healing rates are uniform in the population, the health care provider can track the infection status with the same efficiency, even though the population size increases (while keeping the total infection and healing rates fixed). For the case of λ_i in (80) and μ_i in (81), when we increase the population size, we increase the number of people who rarely become sick, i.e., people with high i indices, and also people who rarely heal from the disease, i.e., people with small i indices. Thus, it becomes easier for the health care provider to track the infection status of the people. This is why when we use λ_i in (80) and μ_i in (81), we observe in Figure 9 that the health care provider can track the infection status of the people better, even though the population size increases.
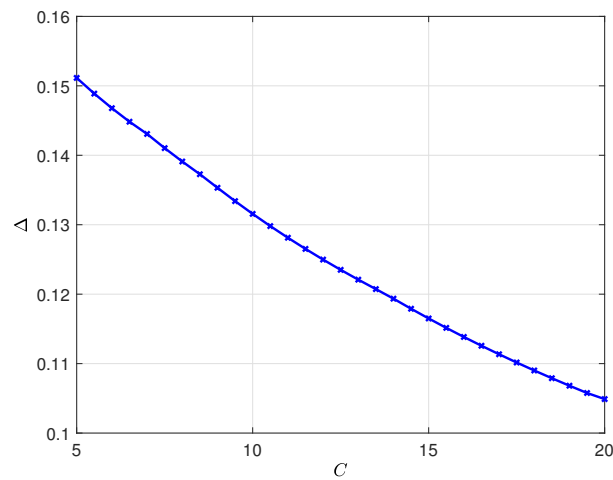
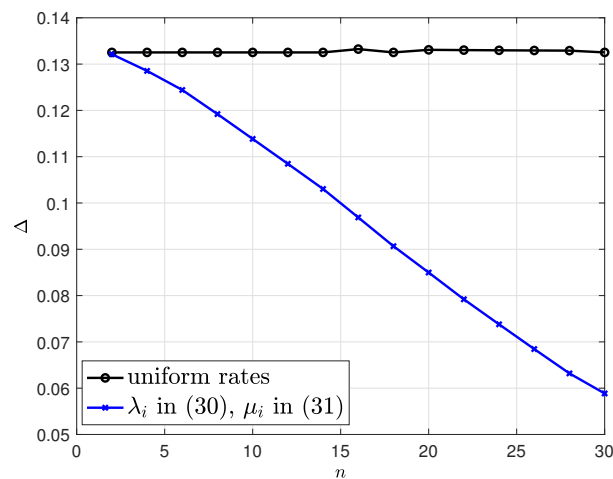**Figure 8.** The average difference Δ with respect to total test rate C.

Figure 9. The average difference Δ with respect to number of people n. We use uniform infection and healing rates, i.e., $\lambda_i = \frac{6}{n}$ and $\mu_i = \frac{4}{n}$ for all i, and also λ_i in (80) and μ_i in (81) with $\sum_{i=1}^{n} \lambda_i = 6$ and $\sum_{i=1}^{n} \mu_i = 4$.

In the fourth example, we employ the same set of variables as the first example except for the importance factor θ. Here, we vary θ in between 0.2 and 0.7. We plot Δ in (7), $\bar{\Delta}_1$ which is $\bar{\Delta}_1 = \frac{1}{n} \sum_{i=1}^{n} \Delta_{i1}$, and $\bar{\Delta}_2$ which is $\bar{\Delta}_2 = \frac{1}{n} \sum_{i=1}^{n} \Delta_{i2}$ in Figure 10a. Note that $\bar{\Delta}_1$ represents the average difference when people are infected, but have not been detected by the health care provider, and $\bar{\Delta}_2$ represents the average difference when people have recovered, but the health care provider still marks them as infected. Note that when θ is high, we assign importance to minimization of $\bar{\Delta}_1$, i.e., the early detection of people with infection, and when θ is low, we give importance to minimization of $\bar{\Delta}_2$, i.e., the early detection of people who recovered from the disease. This is why we observe in Figure 10a that $\bar{\Delta}_1$ decreases with θ while $\bar{\Delta}_2$ increases with θ.

We plot the total test rates $\sum_{i=1}^{n} s_i$ and $\sum_{i=1}^{n} c_i$ in Figure 10b. We observe in Figure 10b that if it is more important to detect the infected people, i.e., if θ is high, then the health care provider should apply higher test rates to people who are marked as healthy. In other words, $\sum_{i=1}^{n} s_i$ increases with θ. Similarly, if it is more important to detect people who recovered from the disease, then the health care provider should apply high test rates to people who are marked as infected. That is, $\sum_{i=1}^{n} c_i$ is high when θ is low. Therefore, depending on the priorities of the health care provider, a suitable θ needs to be chosen.

In the fifth numerical result, we consider the case where there are errors in the test measurements, i.e., the model in Section 5. We take the total test rate as $C = 20$, and vary error rates in the test $p = q = \{0.1, 0.2, 0.4\}$. In Figure 11a, we provide the test rates v_i that we found as a result of our greedy policy in Section 5. When the error rates p and q are low, i.e., when $p = q = 0.1$, we see that the health care provider applies tests to everyone in the population and the corresponding Δ_i^e is lower than applying no test as shown in Figure 11b. As we increase the error rates, we observe that some people in the population start to be not tested by the health care provider, see Figure 11a when $p = q = \{0.2, 0.4\}$. In this case, the health care provider applies more tests to the remaining people to combat the test errors. However, although it applies more tests to the remaining people, we observe in Figure 11b that the achieved average difference Δ_i^e becomes higher as error rates increase.
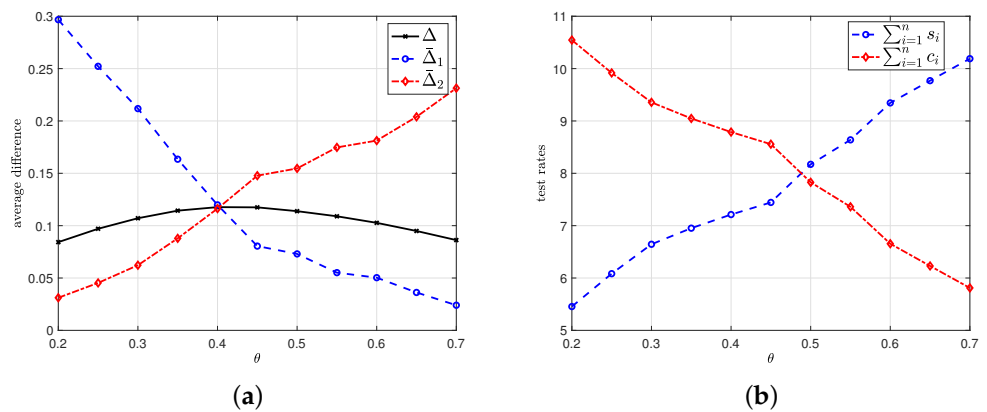

Figure 10. (**a**) Δ in (7), $\bar{\Delta}_1$ which is $\frac{1}{n}\sum_{i=1}^{n}\Delta_{i1}$, and $\bar{\Delta}_2$ which is $\frac{1}{n}\sum_{i=1}^{n}\Delta_{i2}$, (**b**) corresponding total test rates $\sum_{i=1}^{n}s_i$ and $\sum_{i=1}^{n}c_i$.
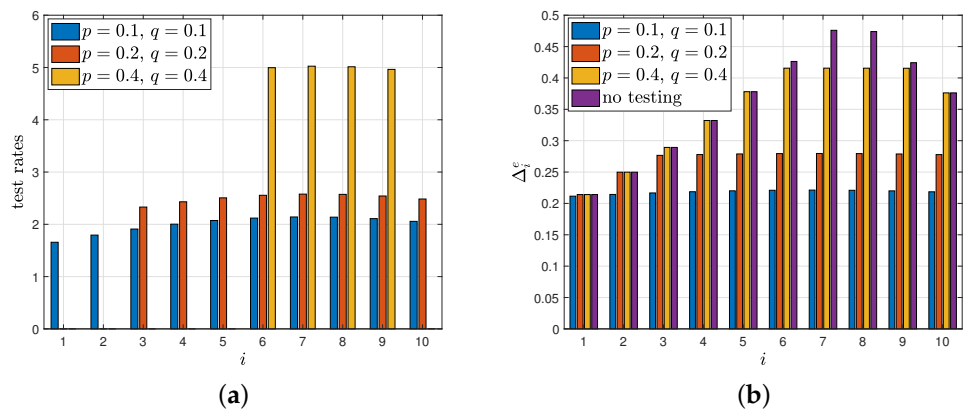

Figure 11. (**a**) Test rates v_i, (**b**) corresponding average difference Δ_i^e when there is error in the tests.

In the sixth numerical result, we consider the case where the infection status of the people depend on each other. In other words, when one person is infected, they can infect the other person with rate λ_{12} when they are not detected by the health care provider, i.e., the infection model in Section 6. For this example, first, we take $\mu = 5$, $\lambda = 2.5$, $s = c = \frac{C}{4}$ and vary $\lambda = \{2, \ldots, 200\}$ and $C = \{20, 40, 60\}$. If $\lambda_{12} = 0$, i.e., if the infection status of people are independent from each other, then the average time that person 1 or 2 is sick is equal to $\frac{\lambda}{\lambda + \mu} = \frac{1}{3}$. As we increase infection rate λ_{12} among the person 1 and 2, we see in Figure 12a that the average time that person 1 is sick increases. However, we note that as we increase the total test rate, the health care provider can detect a sick person more frequently, and this explains why the average infected time is low in Figure 12a when the test rate is high. Then, we consider $\lambda_{12} = \{5, 10, 15\}$ and vary the total test rates $\lambda = \{2, \ldots, 200\}$. We plot the average time that both person 1 and 2 stay as sick in Figure 12b. As we increase the total test rate, the health care provider detects the infected person more quickly, and thus,

prohibits the infection from spreading. As a result, we observe that the average time that both people are infected decreases in C in Figure 12b. Since both people can be infected with the virus independent from each other with rate λ, the plots in Figure 12b do not drop to 0.
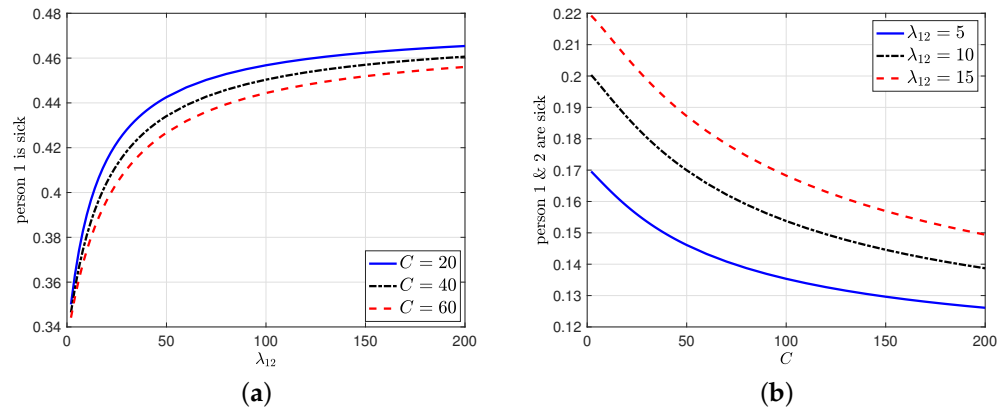

(a)

(b)

Figure 12. (**a**) The percentage of the time that person 1 stays as infected while we increase λ_{12}, (**b**) the percentage of the time that both person 1 and 2 stay as infected while we increase the total test rate C.

In the last numerical result, we consider the age of incorrect information-based error metric in Section 7. Here, the estimation error increases with the time that the health care provider does not detect the changes in the infection status of the people. As a result, the average difference expression given by Δ_i^s in (77) is different than Δ_i^e in (45) when $p = q = 0$. For this example, we consider the total test rate $C = 4$ and compare the normalized average differences given by $\frac{\Delta_i^s}{\sum_{i=1}^n \Delta_i^s}$, and $\frac{\Delta_i^e}{\sum_{i=1}^n \Delta_i^e}$ and the corresponding test rates w_i and v_i. In Figure 13b, depending on the error metric model, people who are tested by the health care provider show considerable variation in their test rates. For example, with the error metric Δ_i^s in (77), we apply tests to every third person while the same person is not tested with the error metric Δ_i^e in (45). In Figure 13a, we provide the normalized average difference values. Here, the average normalized error for the tested people exhibit similar values whereas the normalized difference may vary for the untested people. Thus, we should choose a suitable error metric that satisfies the priorities of the health care provider as it greatly affects who is tested and with which test rates.
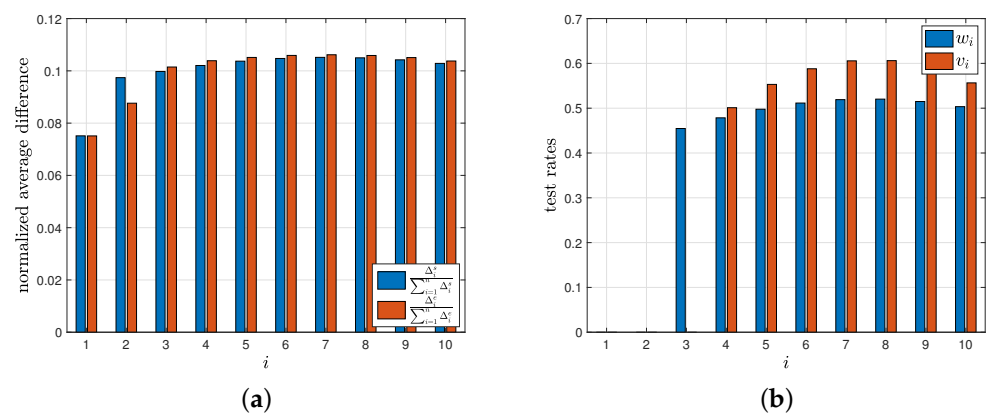

(a)

(b)

Figure 13. (**a**) The normalized average differences $\frac{\Delta_i^s}{\sum_{i=1}^n \Delta_i^s}$, and $\frac{\Delta_i^e}{\sum_{i=1}^n \Delta_i^e}$, and (**b**) the corresponding test rates w_i and v_i.

9. Conclusions and Discussion

We considered the timely tracking of infection status of individuals in a population. For exponential infection and healing processes with given rates, we determined the rates

of exponential testing processes. We considered errors on the test measurements and observed that in order to combat the test errors, a limited portion of the population may be tested with higher test rates. Then, we studied a dependent infection spread model for two people, where one infected person can spread the virus to the other if it has not been detected by the health care provider. Finally, we studied an AoII-based error metric where the error function linearly increases over time as the changes in the infection status have not been detected by the health care provider. We observed in numerical results that the test rates depend on the individuals' infection and recovery rates, the individuals' last known state of being healthy or infected, as well as the health care provider's priorities of detecting infected people versus detecting recovered people more quickly.

In the literature, in order to model epidemics, population is partitioned into groups called *compartments*. One such example is the SIR model used in [106] with the compartments susceptible (S), infected (I), and recovered (R) which has been further developed by adding the states hospitalized (H), and death (D) in [107]. In these epidemic models, the transitions between the compartments are assumed to be Markovian. In [107], with epidemiological data, the delay distributions for the infected (I) to hospitalized (H), and infected (I) to death (D) are well approximated by exponential and gamma distributions, respectively. However, due to the lack of data availability the delay distribution for infected (I) to recovered (R) is modeled with gamma distribution with higher tolerance. In our work, we modeled infection and recovery times, i.e., the delays between recovered (R) to infected (I) and infected (I) to recovered (R) with exponential distributions. Therefore, more realistic infection tracking models can be developed by considering gamma distributions as observed in [107]. This more realistic model corresponds to the problem of real-time timely tracking of a binary Markov source in a serially connected network. The serially connected network model was studied in [8] with the traditional age of information metric. We note that considering the same networking model with the AoII-based error metric to track information dissemination of a binary Markov source represents a promising research direction and has direct applications to the real-time tracking of epidemic spread models. One can also study the extension of dependent infection spread model in Section 6 to $n > 2$ people as a future research direction.

Another interesting research direction could be to consider different kinds of tests with different false-positive and false-negative test rates. Regarding this problem, instead of having a total test rate capacity C, we may consider a total test budget K. Assuming that each test bears a different cost, the goal might be to identify how many tests the health care provider should obtain from each type. Here, one can study a trade-off between applying fewer tests with a small probability of error versus applying more tests to individuals with a high probability of error. Moreover, one can consider a scenario where the health care provider may prefer to apply different test types to individuals depending on their infection and recovery rates.

Author Contributions: Conceptualization, M.B. and S.U.; methodology, M.B. and S.U.; software, M.B.; validation, M.B. and S.U.; formal analysis, M.B. and S.U.; investigation, M.B. and S.U.; resources, M.B. and S.U.; data curation, M.B. and S.U.; writing—original draft preparation, M.B. and S.U.; writing—review and editing, M.B. and S.U.; visualization, M.B. and S.U.; supervision, S.U.; project administration, S.U.; funding acquisition, S.U. All authors have read and agreed to the published version of the manuscript.

Data Availability Statement: Not applicable.

References

1. Kaul, S.K.; Yates, R.D.; Gruteser, M. Real-time status: How often should one update? In Proceedings of the 2012 Proceedings IEEE INFOCOM, Orlando, FL, USA, 25–30 March 2012.
2. Kadota, I.; Sinha, A.; Uysal-Biyikoglu, E.; Singh, R.; Modiano, E. Scheduling policies for minimizing age of information in broadcast wireless networks. *IEEE/ACM Trans. Netw.* **2018**, *26*, 2637–2650. [CrossRef]
3. Kam, C.; Kompella, S.; Nguyen, G.D.; Wieselthier, J.E.; Ephremides, A. Age of information with a packet deadline. In Proceedings of the 2016 IEEE International Symposium on Information Theory (ISIT), Barcelona, Spain, 10–15 July 2016.
4. Sun, Y.; Uysal-Biyikoglu, E.; Yates, R.D.; Koksal, C.E.; Shroff, N.B. Update or wait: How to keep your data fresh. *IEEE Trans. Inf. Theory* **2017**, *63*, 7492–7508. [CrossRef]
5. Najm, E.; Telatar, E. Status updates in a multi-stream M/G/1/1 preemptive queue. In Proceedings of the IEEE Infocom 2018-IEEE Conference On Computer Communications Workshops (Infocom Wkshps), Honolulu, HI, USA, 15–19 April 2018.
6. Soysal, A.; Ulukus, S. Age of information in G/G/1/1 systems: Age expressions, bounds, special cases, and optimization. *IEEE Trans. Inf. Theory* **2021**, *67*, 7477–7489. [CrossRef]
7. Buyukates, B.; Ulukus, S. Age of information with Gilbert-Elliot servers and samplers. *arXiv* **2020**, arXiv:2002.05711.
8. Yates, R.D. The age of information in networks: Moments, distributions, and sampling. *IEEE Trans. Inf. Theory* **2020**, *66*, 5712–5728. [CrossRef]
9. Talak, R.; Karaman, S.; Modiano, E. Minimizing age-of-information in multi-hop wireless networks. In Proceedings of the 2017 55th Annual Allerton Conference on Communication, Control, and Computing (Allerton), Monticello, IL, USA, 3–6 October 2017.
10. Tripathi, V.; Moharir, S. Age of information in multi-source systems. In Proceedings of the GLOBECOM 2017-2017 IEEE Global Communications Conference, Centre, Singapore, 4–8 December 2017.
11. Bedewy, A.M.; Sun, Y.; Shroff, N.B. The age of information in multihop networks. *IEEE/ACM Trans. Netw.* **2019**, *27*, 1248–1257. [CrossRef]
12. Zhong, J.; Yates, R.D.; Soljanin, E. Multicast with prioritized delivery: How fresh is your data? In Proceedings of the 2018 IEEE 19th International Workshop on Signal Processing Advances in Wireless Communications (SPAWC), Kalamata, Greece, 25–28 June 2018.
13. Buyukates, B.; Soysal, A.; Ulukus, S. Age of information in two-hop multicast networks. In Proceedings of the 2018 52nd Asilomar Conference on Signals, Systems, and Computers, Pacific Grove, CA, USA, 28–31 October 2018.
14. Buyukates, B.; Soysal, A.; Ulukus, S. Age of information in multihop multicast networks. *J. Commun. Netw.* **2019**, *21*, 256–267. [CrossRef]
15. Buyukates, B.; Soysal, A.; Ulukus, S. Age of information in multicast networks with multiple update streams. In Proceedings of the 2019 53rd Asilomar Conference on Signals, Systems, and Computers, Pacific Grove, CA, USA, 3–6 November 2019.
16. Krishnan, K.S.A.; Sharma, V. Minimizing age of information in a multihop wireless network. In Proceedings of the ICC 2020-2020 IEEE International Conference on Communications, Dublin, Ireland, 7–11 June 2020.
17. Farazi, S.; Klein, A.G.; Brown, D.R., III. Fundamental bounds on the age of information in multi-hop global status update networks. *J. Commun. Netw.* **2019**, *21*, 268–279. [CrossRef]
18. Ioannidis, S.; Chaintreau, A.; Massoulie, L. Optimal and scalable distribution of content updates over a mobile social network. In Proceedings of the IEEE Infocom, Rio De Janeiro, Brazil, 24 April 2009.
19. Wang, M.; Chen, W.; Ephremides, A. Reconstruction of counting process in real-time: The freshness of information through queues. In Proceedings of the ICC 2019-2019 IEEE International Conference on Communications (ICC), Shanghai, China, 20–24 May 2019.
20. Sun, Y.; Polyanskiy, Y.; Uysal-Biyikoglu, E. Remote estimation of the Wiener process over a channel with random delay. In Proceedings of the 2017 IEEE International Symposium on Information Theory (ISIT), Aachen, Germany, 25–30 June 2017.
21. Sun, Y.; Cyr, B. Information aging through queues: A mutual information perspective. In Proceedings of the 2018 IEEE 19th International Workshop on Signal Processing Advances in Wireless Communications (SPAWC), Kalamata, Greece, 25–28 June 2018.
22. Chakravorty, J.; Mahajan, A. Remote estimation over a packet-drop channel with Markovian state. *IEEE Trans. Autom. Control* **2020**, *65*, 2016–2031. [CrossRef]
23. Kam, C.; Kompella, S.; Ephremides, A. Age of incorrect information for remote estimation of a binary Markov source. In Proceedings of the IEEE INFOCOM 2020-IEEE Conference on Computer Communications Workshops (INFOCOM WKSHPS), Toronto, ON, Canada, 6–9 July 2020.
24. Arafa, A.; Banawan, K.; Seddik, K.G.; Poor, H.V. Sample, quantize and encode: Timely estimation over noisy channels. *IEEE Trans. Commun.* **2021**, *69*, 6485-6499. [CrossRef]
25. Bastopcu, M.; Ulukus, S. Who should Google Scholar update more often? In Proceedings of the IEEE INFOCOM 2020-IEEE Conference on Computer Communications Workshops (INFOCOM WKSHPS), Toronto, ON, Canada, 6–9 July 2020.
26. Bacinoglu, B.T.; Sun, Y.; Uysal-Biyikoglu, E.; Mutlu, V. Achieving the age-energy trade-off with a finite-battery energy harvesting source. In Proceedings of the 2018 IEEE International Symposium on Information Theory (ISIT), Vail, CO, USA, 17–22 June 2018.
27. Baknina, A.; Ozel, O.; Yang, J.; Ulukus, S.; Yener, A. Sending information through status updates. In Proceedings of the 2018 IEEE International Symposium on Information Theory (ISIT), Vail, CO, USA, 17–22 June 2018.
28. Baknina, A.; Ulukus, S. Coded status updates in an energy harvesting erasure channel. In Proceedings of the 2018 52nd Annual Conference on Information Sciences and Systems (CISS), Princeton, NJ, USA, 21–23 March 2018.

29. Wu, X.; Yang, J.; Wu, J. Optimal status update for age of information minimization with an energy harvesting source. *IEEE Trans. Green Commun. Netw.* **2018**, *2*, 193–204. [CrossRef]

30. Feng, S.; Yang, J. Optimal status updating for an energy harvesting sensor with a noisy channel. In Proceedings of the IEEE INFOCOM 2018-IEEE Conference on Computer Communications Workshops (INFOCOM WKSHPS), Honolulu, HI, USA, 15–19 April 2018.

31. Feng, S.; Yang, J. Minimizing age of information for an energy harvesting source with updating failures. In Proceedings of the 2018 IEEE International Symposium on Information Theory (ISIT), Vail, CO, USA, 17–22 June 2018.

32. Arafa, A.; Yang, J.; Ulukus, S.; Poor, H.V. Age-minimal online policies for energy harvesting sensors with incremental battery recharges. In Proceedings of the 2018 Information Theory and Applications Workshop (ITA), San Diego, CA, USA, 11–16 February 2018.

33. Arafa, A.; Yang, J.; Ulukus, S. Age-minimal online policies for energy harvesting sensors with random battery recharges. In Proceedings of the 2018 IEEE international conference on communications (ICC), Kansas City, MO, USA, 20–24 May 2018.

34. Arafa, A.; Yang, J.; Ulukus, S.; Poor, H.V. Age-minimal transmission for energy harvesting sensors with finite batteries: Online policies. *IEEE Trans. Inf. Theory* **2020**, *66*, 534–556. [CrossRef]

35. Arafa, A.; Yang, J.; Ulukus, S.; Poor, H.V. Online timely status updates with erasures for energy harvesting sensors. In Proceedings of the 2018 56th Annual Allerton Conference on Communication, Control, and Computing (Allerton), Monticello, IL, USA, 2–5 October 2018.

36. Arafa, A.; Yang, J.; Ulukus, S.; Poor, H.V. Using erasure feedback for online timely updating with an energy harvesting sensor. In Proceedings of the 2019 IEEE International Symposium on Information Theory (ISIT), Paris, France, 7–12 July 2019.

37. Arafa, A.; Yang, J.; Ulukus, S.; Poor, H.V. Timely status updating over erasure channels using an energy harvesting sensor: Single and multiple sources. *IEEE Trans. Green Commun. Netw.* **2022**, *6*, 6–19. [CrossRef]

38. Farazi, S.; Klein, A.G.; Brown, D.R., III. Average age of information for status update systems with an energy harvesting server. In Proceedings of the IEEE INFOCOM 2018-IEEE Conference on Computer Communications Workshops (INFOCOM WKSHPS), Honolulu, HI, USA 15–19 April 2018.

39. Leng, S.; Yener, A. Age of information minimization for an energy harvesting cognitive radio. *IEEE Trans. Cogn. Commun. Netw.* **2019**, *5*, 427–439. [CrossRef]

40. Chen, Z.; Pappas, N.; Bjornson, E.; Larsson, E.G. Age of information in a multiple access channel with heterogeneous traffic and an energy harvesting node. In Proceedings of the IEEE INFOCOM 2019-IEEE Conference on Computer Communications Workshops (INFOCOM WKSHPS), Paris, France, 29 April–2 May 2019.

41. Bhat, R.V.; Vaze, R.; Motani, M. Throughput maximization with an average age of information constraint in fading channels. *IEEE Trans. Wirel. Commun.* **2021**, *20*, 481–494. [CrossRef]

42. Ostman, J.; Devassy, R.; Durisi, G.; Uysal, E. Peak-age violation guarantees for the transmission of short packets over fading channels. In Proceedings of the IEEE INFOCOM 2019-IEEE Conference on Computer Communications Workshops (INFOCOM WKSHPS), Paris, France, 29 April–2 May 2019.

43. Bastopcu, M.; Ulukus, S. Age of information with soft updates. In Proceedings of the 2018 56th Annual Allerton Conference on Communication, Control, and Computing (Allerton), Monticello, IL, USA, 2–5 October 2018.

44. Bastopcu, M.; Ulukus, S. Minimizing age of information with soft updates. *J. Commun. Netw.* **2019**, *21*, 233–243. [CrossRef]

45. Buyukates, B.; Soysal, A.; Ulukus, S. Age of information scaling in large networks. In Proceedings of the 2019 IEEE Global Communications Conference (GLOBECOM), Waikoloa, HI, USA, 9–13 December 2019.

46. Buyukates, B.; Soysal, A.; Ulukus, S. Age of information scaling in large networks with hierarchical cooperation. In Proceedings of the 2019 IEEE Global Communications Conference (GLOBECOM), Waikoloa, HI, USA, 9–13 December 2019.

47. Buyukates, B.; Soysal, A.; Ulukus, S. Scaling laws for age of information in wireless networks. *IEEE Trans. Wirel. Commun.* **2021**, *20*, 2413–2427. [CrossRef]

48. Zhong, J.; Yates, R.D.; Soljanin, E. Minimizing content staleness in dynamo-style replicated storage systems. In Proceedings of the IEEE INFOCOM 2018-IEEE Conference on Computer Communications Workshops (INFOCOM WKSHPS), Honolulu, HI, USA, 15–19 April 2018.

49. Rajaraman, N.; Vaze, R.; Reddy, G. Not just age but age and quality of information. *IEEE J. Sel. Areas Commun.* **2021**, *39*, 1325–1338. [CrossRef]

50. Liu, Z.; Ji, B. Towards the tradeoff between service performance and information freshness. In Proceedings of the ICC 2019-2019 IEEE International Conference on Communications (ICC), Shanghai, China, 20–24 May 2019.

51. Maatouk, A.; Assaad, M.; Ephremides, A. The age of incorrect information: An enabler of semantics-empowered communication. *arXiv* **2020**, arXiv:2012.13214.

52. Uysal, E.; Kaya, O.; Ephremides, A.; Gross, J.; Codreanu, M.; Popovski, P.; Johansson, K.H. Semantic communications in networked systems. *arXiv* **2021**, arXiv:2103.05391.

53. Ayan, O.; Vilgelm, M.; Klügel, M.; Hirche, S.; Kellerer, W. Age-of-information vs. value-of-information scheduling for cellular networked control systems. In Proceedings of the 10th ACM/IEEE International Conference on Cyber-Physical Systems, Montreal, QC, Canada, 16–18 April 2019.

54. Bastopcu, M.; Ulukus, S. Timely group updating. In Proceedings of the 2021 55th Annual Conference on Information Sciences and Systems (CISS), Baltimore, MD, USA, 24–26 March 2021.

55. Banerjee, S.; Bhattacharjee, R.; Sinha, A. Fundamental limits of age-of-information in stationary and non-stationary environments. In Proceedings of the 2020 IEEE International Symposium on Information Theory (ISIT), Los Angeles, CA, USA, 21–26 June 2020.

56. Zhong, J.; Yates, R.D. Timeliness in lossless block coding. In Proceedings of the 2016 Data Compression Conference (DCC), Snowbird, UT, USA, 29 March–1 April 2016.

57. Zhong, J.; Yates, R.D.; Soljanin, E. Timely lossless source coding for randomly arriving symbols. In Proceedings of the 2018 IEEE Information Theory Workshop (ITW), Guangzhou, China, 25–29 November 2018.

58. Mayekar, P.; Parag, P.; Tyagi, H. Optimal lossless source codes for timely updates. In Proceedings of the 2018 IEEE International Symposium on Information Theory (ISIT), Vail, CO, USA, 17–22 June 2018.

59. Mayekar, P.; Parag, P.; Tyagi, H. Optimal source codes for timely updates. *IEEE Trans. Inf. Theory* **2020**, *66*, 3714–3731. [CrossRef]

60. Bastopcu, M.; Buyukates, B.; Ulukus, S. Optimal selective encoding for timely updates. In Proceedings of the 2020 54th Annual Conference on Information Sciences and Systems (CISS), Princeton, NJ, USA, 18–20 March 2020.

61. Buyukates, B.; Bastopcu, M.; Ulukus, S. Optimal selective encoding for timely updates with empty symbol. In Proceedings of the 2020 IEEE International Symposium on Information Theory (ISIT), Los Angeles, CA, USA, 21–26 June 2020.

62. Bastopcu, M.; Buyukates, B.; Ulukus, S. Selective encoding policies for maximizing information freshness. *IEEE Trans. Commun.* **2021**, *69*, 5714–5726. [CrossRef]

63. Ramirez, D.; Erkip, E.; Poor, H.V. Age of information with finite horizon and partial updates. In Proceedings of the ICASSP 2020-2020 IEEE International Conference on Acoustics, Speech and Signal Processing (ICASSP), Barcelona, Spain, 4–8 May 2020.

64. Arafa, A.; Banawan, K.; Seddik, K.G.; Poor, H.V. On timely channel coding with hybrid ARQ. In Proceedings of the 2019 IEEE Global Communications Conference (GLOBECOM), Big Island, HI, USA, 9–13 December 2019.

65. Arafa, A.; Wesel, R.D. Timely transmissions using optimized variable length coding. In Proceedings of the IEEE INFOCOM 2021-IEEE Conference on Computer Communications Workshops (INFOCOM WKSHPS), Vancouver, BC, Canada, 10–13 May 2021.

66. Bastopcu, M.; Ulukus, S. Partial updates: Losing information for freshness. In Proceedings of the 2020 IEEE International Symposium on Information Theory (ISIT), Los Angeles, CA, USA, 21–26 June 2020.

67. Abd-Elmagid, M.A.; Dhillon, H.S. Average peak age-of-information minimization in UAV-assisted IoT networks. *IEEE Trans. Veh. Technol.* **2019**, *68*, 2003–2008. [CrossRef]

68. Liu, J.; Wang, X.; Dai, H. Age-optimal trajectory planning for UAV-assisted data collection. In Proceedings of the IEEE INFOCOM 2018-IEEE Conference on Computer Communications Workshops (INFOCOM WKSHPS), Honolulu, HI, USA, 15–19 April 2018.

69. Abd-Elmagid, M.A.; Pappas, N.; Dhillon, H.S. On the role of age of information in the internet of things. *IEEE Commun. Mag.* **2019**, *57*, 72–77. [CrossRef]

70. Alabbasi, A.; Aggarwal, V. Joint information freshness and completion time optimization for vehicular networks. *IEEE Trans. Serv. Comput.* **2020**, *15*, 1–14. [CrossRef]

71. Gao, W.; Cao, G.; Srivatsa, M.; Iyengar, A. Distributed maintenance of cache freshness in opportunistic mobile networks. In Proceedings of the 2012 IEEE 32nd International Conference on Distributed Computing Systems, Macau, China, 18–21 June 2012.

72. Yates, R.D.; Ciblat, P.; Yener, A.; Wigger, M. Age-optimal constrained cache updating. In Proceedings of the 2017 IEEE International Symposium on Information Theory (ISIT), Aachen, Germany, 25–30 June 2017.

73. Kam, C.; Kompella, S.; Nguyen, G.D.; Wieselthier, J.E.; Ephremides, A. Information freshness and popularity in mobile caching. In Proceedings of the 2017 IEEE International Symposium on Information Theory (ISIT), Aachen, Germany, 25–30 June 2017.

74. Zhang, S.; Li, J.; Luo, H.; Gao, J.; Zhao, L.; Shen, X.S Towards fresh and low-latency content delivery in vehicular networks: An edge caching aspect. In Proceedings of the 2018 10th International Conference on Wireless Communications and Signal Processing (WCSP), Hangzhou, China, 18–20 October 2018.

75. Tang, H.; Ciblat, P.; Wang, J.; Wigger, M.; Yates, R. Age of information aware cache updating with file- and age-dependent update durations. In Proceedings of the 2020 18th International Symposium on Modeling and Optimization in Mobile, Ad Hoc, and Wireless Networks (WiOPT), Volos, Greece, 15–19 June 2020.

76. Zhong, J.; Yates, R.D.; Soljanin, E. Two freshness metrics for local cache refresh. In Proceedings of the 2018 IEEE International Symposium on Information Theory (ISIT), Vail, CO, USA, 17–22 June 2018.

77. Yang, L.; Zhong, Y.; Zheng, F.; Jin, S. Edge caching with real-time guarantees. *arXiv* **2019**, arXiv:1912.11847.

78. Bastopcu, M.; Ulukus, S. Maximizing information freshness in caching systems with limited cache storage capacity. In Proceedings of the 2020 54th Asilomar Conference on Signals, Systems, and Computers, Pacific Grove, CA, USA, 1–5 November 2020.

79. Bastopcu, M.; Ulukus, S. Cache freshness in information updating systems. In Proceedings of the 2021 55th Annual Conference on Information Sciences and Systems (CISS), Baltimore, MD, USA, 24–26 March 2021.

80. Bastopcu, M.; Ulukus, S. Information freshness in cache updating systems. *IEEE Trans. Wirel. Commun.* **2021**, *20*, 1861–1874. [CrossRef]

81. Kaswan, P.; Bastopcu, M.; Ulukus, S. Freshness based cache updating in parallel relay networks. In Proceedings of the 2021 IEEE International Symposium on Information Theory (ISIT), Melbourne, Australia, 12–20 July 2021.

82. Gu, Y.; Wang, Q.; Chen, H.; Li, Y.; Vucetic, B. Optimizing information freshness in two-hop status update systems under a resource constraint. *IEEE J. Sel. Areas Commun.* **2021**, *39*, 1380–1392. [CrossRef]

83. Kuang, Q.; Gong, J.; Chen, X.; Ma, X. Age-of-information for computation-intensive messages in mobile edge computing. *arXiv* **2019**, arXiv:1901.01854.

84. Gong, J.; Kuang, Q.; Chen, X.; Ma, X. Reducing age-of-information for computation-intensive messages via packet replacement. In Proceedings of the 2019 11th International Conference on Wireless Communications and Signal Processing (WCSP), Xi'an, China, 23–25 October 2019.

85. Zou, P.; Ozel, O.; Subramaniam, S. Trading off computation with transmission in status update systems. In Proceedings of the 2019 IEEE 30th Annual International Symposium on Personal, Indoor and Mobile Radio Communications (PIMRC), Istanbul, Turkey, 8–11 September 2019.

86. Bastopcu, M.; Ulukus, S. Age of information for updates with distortion. In Proceedings of the 2019 IEEE Information Theory Workshop (ITW), Gotland, Sweden, 25–28 August 2019.

87. Bastopcu, M.; Ulukus, S. Age of information for updates with distortion: Constant and age-dependent distortion constraints. *IEEE/ACM Trans. Netw.* **2021**, *29*, 2425–2438. [CrossRef]

88. Buyukates, B.; Ulukus, S. Timely updates in distributed computation systems with stragglers. In Proceedings of the 2020 54th Asilomar Conference on Signals, Systems, and Computers, Pacific Grove, CA, USA, 1–5 November 2020.

89. Buyukates, B.; Ulukus, S. Timely distributed computation with stragglers. *IEEE Trans. Commun.* **2020**, *68*, 5273–5282. [CrossRef]

90. Zou, P.; Ozel, O.; Subramaniam, S. Optimizing information freshness through computation–transmission tradeoff and queue management in edge computing. *IEEE/ACM Trans. Netw.* **2021**, *29*, 949–963. [CrossRef]

91. Buyukates, B.; Ulukus, S. Timely communication in federated learning. In Proceedings of the IEEE INFOCOM 2021-IEEE Conference on Computer Communications Workshops (INFOCOM WKSHPS), Vancouver, BC, Canada, 10–13 May 2021.

92. Ozfatura, E.; Buyukates, B.; Gündüz, D.; Ulukus, S. Age-based coded computation for bias reduction in distributed learning. In Proceedings of the GLOBECOM 2020-2020 IEEE Global Communications Conference, Taipei, Taiwan, 7–11 December 2020.

93. Ceran, E.T.; Gündüz, D.; György, A. A reinforcement learning approach to age of information in multi-user networks with HARQ. *IEEE J. Sel. Areas Commun.* **2021**, *39*, 1412–1426. [CrossRef]

94. Yates, R.D. The age of gossip in networks. In Proceedings of the 2021 IEEE International Symposium on Information Theory (ISIT), Melbourne, Australia, 12–20 July 2021.

95. Buyukates, B.; Bastopcu, M.; Ulukus, S. Age of gossip in networks with community structure. In Proceedings of the 2021 IEEE 22nd International Workshop on Signal Processing Advances in Wireless Communications (SPAWC), Lucca, Italy, 27–30 September 2021.

96. Bastopcu, M.; Buyukates, B.; Ulukus, S. Gossiping with binary freshness metric. In Proceedings of the 2021 IEEE Globecom Workshops (GC Wkshps), Madrid, Spain, 7–11 December 2021.

97. Kaswan, P.; Ulukus, S. Timely gossiping with file slicing and network coding. *arXiv* **2022**, arXiv:2202.00649.

98. Kosta, A.; Pappas, N.; Angelakis, V. Age of information: A new concept, metric, and tool. *Found. Trends Netw.* **2017**, *12*, 162–259. [CrossRef]

99. Sun, Y.; Kadota, I.; Talak, R.; Modiano, E. Age of information: A new metric for information freshness. *Synth. Lect. Commun. Netw.* **2019**, *12*, 1–224. [CrossRef]

100. Yates, R.D.; Sun, Y.; Brown, D.R., III; Kaul, S.K.; Modiano, E.; Ulukus, S. Age of information: An introduction and survey. *IEEE J. Sel. Areas Commun.* **2021**, *39*, 1183–1210. [CrossRef]

101. Yun, J.; Joo, C.; Eryilmaz, A. Optimal real-time monitoring of an information source under communication costs. In Proceedings of the 2018 IEEE Conference on Decision and Control (CDC), Miami Beach, FL, USA, 17–19 December 2018.

102. Maatouk, A.; Kriouile, S.; Assaad, M.; Ephremides, A. The age of incorrect information: A new performance metric for status updates. *IEEE/ACM Trans. Netw.* **2020**, *28*, 2215–2228. [CrossRef]

103. Yates, R.D.; Goodman, D.J. *Probability and Stochastic Processes*; Wiley: Hoboken, NJ, USA, 2014.

104. Boyd, S.P.; Vandenberghe, L. *Convex Optimization*; Cambridge University Press: Cambridge, UK, 2004.

105. Bertsekas, D.P.; Tsitsiklis, J.N. *Introduction to Probability*; Athena Scientific: Belmont, MA, USA, 2008.

106. Chen, Y.C.; Lu, P.E.; Chang, C.S.; Liu, T.H. A time-dependent SIR model for COVID-19 with undetectable infected persons. *IEEE Trans. Netw. Sci. Eng.* **2020**, *7*, 3279–3294. [CrossRef]

107. Olmez, S.Y.; Mori, J.; Miehling, E.; Başar, T.; Smith, R.L.; West, M.; Mehta, P.G. A data-informed approach for analysis, validation, and identification of COVID-19 models. In Proceedings of the 2021 American Control Conference (ACC), New Orleans, LA, USA, 25–28 May 2021.